CHALMERS
UNIVERSITY OF TECHNOLOGY

Empirical Prediction of Ground-Borne Vibration from Railway Systems

Validating the HS2 model in Sweden, west coast.

Master's thesis in Sound and Vibration

JIM NORDSTRÖM

DEPARTMENT OF APPLIED ACOUSTICS

CHALMERS UNIVERSITY OF TECHNOLOGY
Gothenburg, Sweden 2023
www.chalmers.se

Master's thesis 2023

Empirical Prediction of Ground-Borne Vibration from Railway Systems

JIM NORDSTRÖM

CHALMERS
UNIVERSITY OF TECHNOLOGY

Department of Architecture and Civil Engineering
Division of Applied Acoustics
Chalmers University of Technology
Gothenburg, Sweden 2023

Empirical Prediction of Ground-Borne Vibration from Railway Systems
JIM NORDSTRÖM

Supervisor: Mats Hammarqvist, Efterklang - part of AFRY
Examiner: Patrik Höstmad, Department of Architecture and Civil Engineering

Master's Thesis ACEX30 2023
Department of Architecture amd Civil Engineering
Division of Applied Acoustics
Chalmers University of Technology
SE-412 96 Gothenburg
Telephone +46 31 772 1000

Cover: Ett SJ2000 tåg mot Sundsvall vid G:a Uppsala sept 2010. Picture acquired from [2].

Typeset in LaTeX
Gothenburg, Sweden 2023

Empirical Prediction of Ground-Borne Vibration from Railway Systems
JIM NORDSTRÖM
Department of Applied Acoustics
Chalmers University of Technology

Abstract

Trains are becoming a more and more viable option as a fast, environmentally friendly travel choice. Along with this cities grows larger and civilizations becomes more urbanised. This results in an increase of human exposure to vibrations from trains, creating a need of vibration level predictions. Predictions enables at an early stage to be able to tell the impact of a new railway system. Whether residence buildings can be built at a certain proximity to the rail or hospitals, research facilities with vibration sensitive instruments, what trains with what speeds can pass and so on. One model to do this is the British empirical model named High Speed 2 (HS2). In Sweden, especially the west coast, the lithology differs from that of the UK as a result of the melting glaciers. Soft ground material, such as the Swedish glacial clay have tendencies to generate low frequency vibrational disturbances.

This thesis is an evaluation of the HS2 model under Swedish conditions. It is limited to predicting the vibration levels in the ground at a certain distance from a surface running train. In 2021 a thesis work of Gustav Vågfelt was done were the HS2 model was implemented in Matlab and evaluated against a measurement data set at a Swedish site with help of Efterklang - part of AFRY [1] [15]. This thesis will continue on that work and in cooperation with Efterklang use the Matlab implementation to evaluate the model by conducting measurements at two different sites, one being post glacial fine sand and the other glacial clay. As there are still uncertainties in the model parameters a final conclusion of its precision can not yet be set. With the data available however the HS2 performs decent on the fine sand with quite consistent results and with the evaluation tools a table of values presenting the expected precision of the model is presented. The HS2 model did however not perform as well on the glacial clay. Because of this it was extended with an additional lithology to fit the Swedish glacial clay. This lithology performed excellent for the glacial clay site measurements, however that is expected as it originated from them. It was also tested on external measurement data from Greby, Skövde which also consisted of glacial clay. Here the extension of the model was less accurate. This indicates that measurement data from more glacial clay ground sites are needed to get a more accurate model extension.

Keywords: Ground-Borne Noise and Vibration, High-speed Trains, Railway Systems, High-Speed 2 (HS2) Prediction Model, Empirical, Model Evaluation, Low Frequency Vibration, Soft Ground Materials, Glacial Clay.

Acknowledgements

I would like to express my gratitude to Mats Hammarqvist and Gustav Vågfelt from Efterklang for their support and assistance throughout this project. Mats' organizational skills and guidance were instrumental in ensuring the success of this study, while Gustav's availability and support, no matter how big or small the issue, were truly appreciated.

Jim Nordström, Gothenburg, 03 2023

Contents

1
Introduction

The subject of noise and vibrations is something that has been greatly elevated over the last years. As civilization grows and evolves so does its potential to damage buildings, the environment, animals and humans. With this the need to create a safer and more comfortable surrounding grows as well. Within the scope of this subject lays ground vibrations. Sources of ground vibrations can be naturally occurring, such as an earthquake, but is most often the result of man-made acts. This includes construction work, e.g. piling, drilling, blasting, dynamic compaction as well as operating heavy construction equipment. It also includes road and railway transportation, the latter of which is the focused source of vibrations in this thesis.

Today, to encourage traveling by train, residences are built in proximity to train stations [18]. Partly because of this, a lot of houses today are positioned close to roads and railways. As the weight and speed of our transporting vehicles increases so does the vibrations. In the case of railway the main source of vibrations is the trains weight on the rail pushing down on the ground, where all the interactions between the train and rail are to be considered. This includes the surface roughness of the wheels and the rail as well as track type and train design. The transmission path, both by geometrical and material factors also highly impacts the vibrations. The transmission path is often not very homogeneous and can be hard to accurately describe with a combination of different types of soil and rock. All in all the process of a ground vibration from a source to a receiver is a complex process depending on a large number of factors.

A powerful tool for facing complex problems such as this, is the empirical model. By using a large amount of ground-borne vibration measurements from railway good models can be acquired. By accounting for sufficiently amount of factors, including the ones mentioned above, accurate predictions can then be done. One such model is the High Speed 2 (HS2) model [10]. The model was developed in the United Kingdom using data from thousands of measurements from trains. It is applicable on multiple train types, speeds, different geological profiles, trains running on surface ground as well as in bored train tunnels and the predictions are generally proven accurate. Validation of the model was done in Germany as well as France and when comparing it to the abroad measurements it was realized how large the geological conditions impacted the vibrations [5].

In 2021, a master thesis by Gustav Vågfelt at Chalmers university of technology was done where the HS2 model was tested under Swedish conditions. The model was

implemented in Matlab and predictions were tested against a measurement done in Sweden. The accuracy of the model was relatively good, however some parameters from the measurements needed for the model was not available and the model needs more measurements for validation. This master thesis will continue the work of Gustav Vågfelt and validate as well as extend the model for Swedish conditions. Mainly the geological profile of Sweden is different then that of previous validation locations, but all the parameters need to be calibrated to Swedish conditions. In order to fulfill this in-situ measurements of ground-borne vibrations needs to be done and a sufficiently amount of data needs to be gathered in order to, not only validate the model, but also legitimize any extensions of it, e.g. add a Swedish geological profile.
The thesis will be conducted with the acoustics department of AFRY, Efterklang [15].

1.1 Aim and Objectives

The aim of this thesis is to validate the HS2 model under Swedish circumstances. This is done by doing multiple measurements of ground-borne vibrations as well as using and extending the Matlab implementation of the HS2 model. The predictions from the model will then be tested against the measured data and the results evaluated.

1. Study the fundamental physics of ground vibrations as well as study the specific field of ground-borne vibrations from trains.
2. Study the HS2 model and its implementation in Matlab.
3. Learn the parameters used in the model and research them for the measurements to be done.
4. Plan and perform measurements. During the measurements further input data for the HS2 model must be acquired as well.
5. Use the Matlab model to make predictions of vibrations and compare that with the measurements. Analyse the results. Answer the questions: What is an accurate prediction? How accurate can the model predict?
6. Expand and/or adjust the model to further adapt it for Swedish conditions. Verify the expansion/adjustment.

1.2 Demarcations

As this thesis will touch on multiple subjects demarcations of the scope are important to set.

- Only ground-borne vibrations will be taken into account in this project, not air-borne.
- Only surface driven trains will be taken into account.
- The measurements will be done on two different soil types in western Sweden. This is not characteristic for the entire country, nor all soil of the same soil type.

2
Theory

This section will describe the fundamental theory of the transmission of ground-borne vibrations necessary for the prediction model. The process can be divided into three phases, each of them distinct with its own effects on the vibrations magnitude, time period and frequency content. They are the vibrations source, the propagation and the receiver.

The first phase is the characteristics of the vibration *source* and is further explained in section 2.1. It describes the excitation that occurs from the interaction of a moving train together with its wheels, the track as well as the infrastructure supporting it. All these parameters will modify and transfer the vibration into the surrounding soil. The second phase is the *propagation* phase, see section 2.2. The vibrations will travel as waves, either along the surface or down in all directions in the ground. As it propagates through the ground it will be affected by material damping and geometrical attenuation factors depending on properties of the medium (soil) and how far it propagates. A section about geology and geophysics will also be included explaining fundamentals of geology and properties of some generic ground material types. The last phase is the *receiver*, see section 2.3. The section will describe the human response to vibrations as well as the impact it has on buildings. The ground-borne waves reach the foundation of a building, creating movements in it that will spread through the construction. Every element reacts in its own way, and the resulting vibrations could cause damage to the building, cause noise or in other ways be disturbing for people in the building.
An example process with outlined phases is presented in figure 2.1.

2.1 Vibration sources, train wheels

The Swedish railway network consists of around 15 600 km of track [23]. On this track a wide variety of trains are traveling, with different length, load, speed etc. The geometrical structures of the railway embankments differ and are built upon different ground types varying from bedrock to loose clay, peat or mud. Besides this the rail quality is highly changing as well. All these parameters and all their different combinations makes estimating ground vibrations a complex process. There are a number of factors affecting the emission of waves from a train, a few of them just mentioned above.

The main source of railway induced vibrations are the moving distortion of the rail

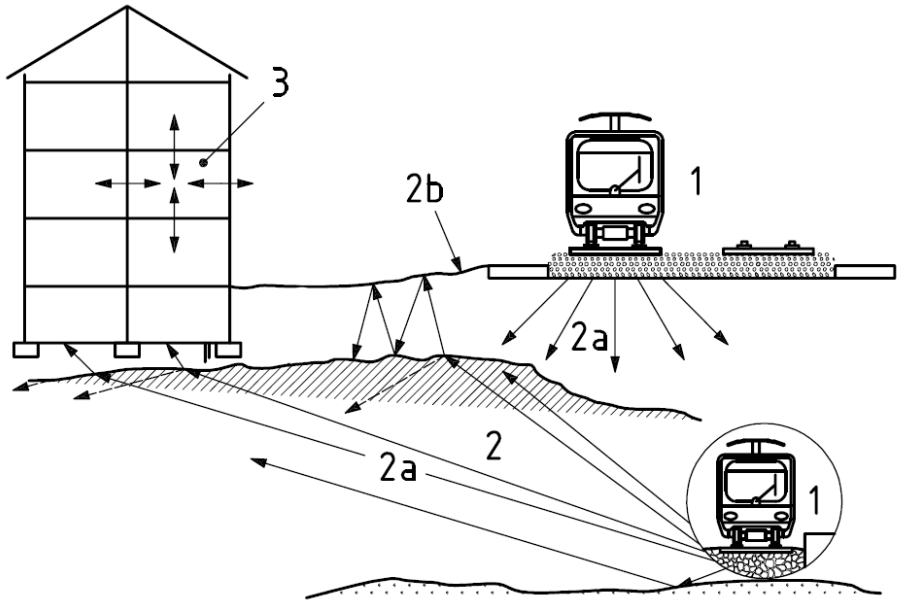

Figure 2.1: Example of ground-borne vibration process starting from a source (1), the transmission path (2) and the receiver (3). 2a represents body waves and 2b surface waves. Reprinted with permission from [19].

structure that comes from the load of the moving train, as is visualised in figure 2.2. A train has its contact points under the wheels, i.e. a small area where all the gravitation force is concentrated, resulting in a displacement of the rail with supporting infrastructure, which is exaggerated in the figure. As the force moves along the rail so does the displacement or rather; at a fixed location a time dependant deformation occurs which in turn excite waves into the track and ground. The speed of the train will then determine the frequency of the excitation, most often related to low frequent vibrations. Additionally, for tracks with discrete rail support, such as the traditional setup with sleepers on ballast, the supporting track will have a varying stiffness depending on its distance to a sleeper. In a similar manner there will be harmonic components excited due to axle and bogie spacing. This means that the dimensions of the train and track are important parameters for ground-borne vibrations. A presentation of relevant dimensions which will later on be used in the HS2-model, see section 3, are presented in figure 3.3.

Other then the main source there are many factors that will have an impact. Every imbalance of the train or unevenness of the track may cause forces giving rise to vibrations in the ground. Acceleration or retardation of the train can also do it. Wheels may be defect or the train boogies unbalanced creating repetitive forces into the ground. Roughness on the wheel or rail, i.e. irregularities of the contact surfaces, can lead to excitations. There may be more severe roughness as a result of operation, e.g. corrugation. On wheels corrugation may occur with other severe

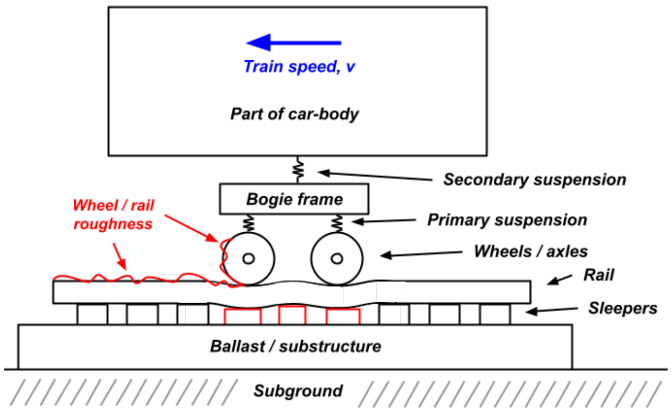

Figure 2.2: Example model of train track interaction. Reprinted with permission from [1].

irregularities such as wheel flats, ovality or eccentricity. The rail can be unbalanced, sleepers can miss contact with the ballast or the subgrade can have a varying depth and stiffness. The remedial grinding of the track can also be insufficient or inappropriate in case of corrugated track. Furthermore the neighboring ground will have natural variations and not be fully homogeneous with materials of varying stiffness and depth. Especially loose subground, such as can be found around the west coast of Sweden, is known to give rise to large vibrations. Each one of these sources will create ground-borne vibrations spreading to the surrounding. Some of the sources are locally geographically bound while some will create a repetitive force inducing pattern moving along the train.

2.2 Transmission path

After the source gives rise to movements in the ground these movements will travel via the transmission path, from the rail structure into the underlying ground to a receiver. The vibrations are travelling mainly as three different types of waves: compression waves (longitudinal waves, P-waves, primary waves), shear waves (secondary waves, S-waves) and surface waves (Rayleigh waves or Love waves). This section will explain the theory of the wave types that occurs in ground during vibrations in further detail. A technical section about relevant technical geology is also explained in section 2.2.3.

2.2.1 Elastic waves in solid materials

The first type of waves are the body waves. These are the waves that moves through the interior of the earth and includes longitudinal waves and shear waves. As they propagate in all directions in the ground (more or less, depending on the homogeneity of the ground) they will be more attenuated compared to the surface waves. This

is of both geometrical and material damping reasons.

The longitudinal wave is defined as a wave for which the vibrating particles of the medium is moving parallel to the direction of propagation. When dealing with mechanical waves it is also known as a compression wave or p-wave (pressure wave or primary wave), since the medium experiences compression/rarefaction and pressure changes as the wave propagates through it. The waveform and how it affects the medium is presented in figure 2.3.

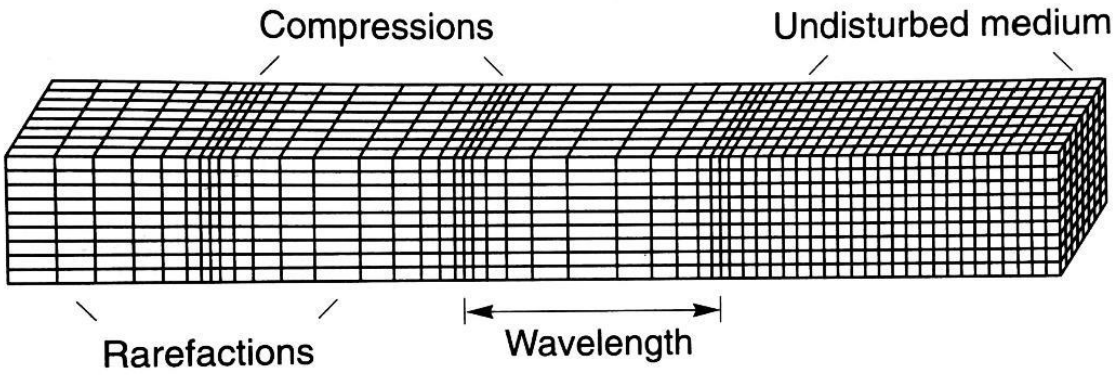

Figure 2.3: Motion of medium during longitudinal wave propagation. Reprinted with permission from [20].

The propagation speed (m/s) of the p-wave is dependant on medium properties and can be determined by

$$c_p = \sqrt{\frac{E(1-\nu)}{\rho(1-2\nu)(1+\nu)}}, \tag{2.1}$$

where E is the Young's modulus (Pa) of the medium, ν is the Poisson's ratio and ρ is the density (kg/m^3) of the medium. The longitudinal wave propagates mostly downwards into the ground (or radially for tunnels), shown as 2a in figure 2.1. The velocity of the propagation depends on the grounds density, where higher density means higher velocity. The typical velocity range for longitudinal waves in soil are around 800 to 2000 m/s (1500 m/s in water) and are as such the fastest ground-borne wave type and often the one to be felt first, hence the name primary wave.

The other body wave is the shear wave or s-wave (secondary wave). This, in contrast to the longitudinal wave is a transverse wave, meaning the vibrating particles in the medium has a movement perpendicular to the wave propagation direction. The motion of a medium exposed to shear waves are presented in figure 2.4.

The speed (m/s) of the shear wave is calculated by

$$c_s = \sqrt{\frac{G}{\rho}} = \sqrt{\frac{E}{\rho 2(1+\nu)}}, \tag{2.2}$$

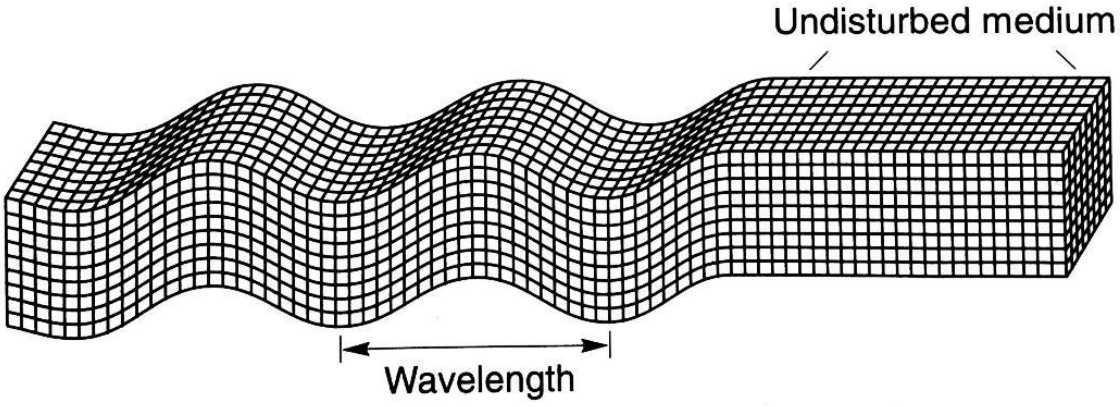

Figure 2.4: Motion of medium during shear wave propagation. Reprinted with permission from [20].

where G is the shear modulus (Pa), ρ is the density (kg/m^3), E is the Young's modulus (Pa) and ν is the Poisson's ratio.

Along free surfaces another type of wave can propagate; the surface wave. The surface wave is the result of the interaction between body waves, the ground surface and the upper soil layers. They travel along the ground surface with a strongly decreasing amplitude over depth, mainly noticeable around one wavelength in depth. In terms of excitation of buildings the surface waves are often the most relevant wave type. The Rayleigh wave is the most common surface wave and another relevant but less occurring surface wave is the Love wave.

The Rayleigh wave is a combination of a longitudinal and transversal wave and the particle movement of the medium is in principle elliptical, as can be seen in figure 2.5. The speed (m/s) of the Rayleigh is approximated as follows:

$$c_R \approx \frac{0.87 + 1.12\nu}{1 + \nu} c_s, \tag{2.3}$$

where ν is Poisson's ratio and c_s is the speed of the secondary wave.

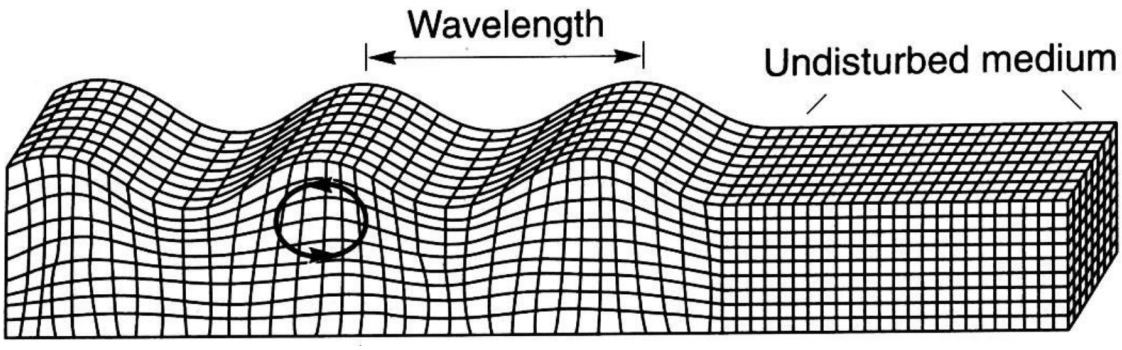

Figure 2.5: Motion of medium during Rayleigh wave propagation. Reprinted with permission from [20].

The less occurring Love wave will only arise if the top soil layer has lower stiffness than the lower layer. The movement of the wave is described as a horizontal shear wave that is "stuck" in the upper layer of the ground, as seen in figure 2.6 where the top layer deforms horizontally. The propagation speed may vary between the speed of the shear wave in the upper layer during high frequencies (c_{s1}) and the lower layer during low frequencies (c_{s2}) according to:

$$c_L = tan(2\pi f\sqrt{\frac{1}{{c_{s1}}^2} - \frac{1}{{c_L}^2}}) = \frac{{c_{s2}}^2\rho_2\sqrt{1/{c_L}^2 - 1/{c_{s2}}^2}}{{c_{s1}}^2\rho_1\sqrt{1/{c_{s1}}^2 - 1/{c_L}^2}}, \tag{2.4}$$

where f is the frequency and ρ_i is the soil density for each respective layer.

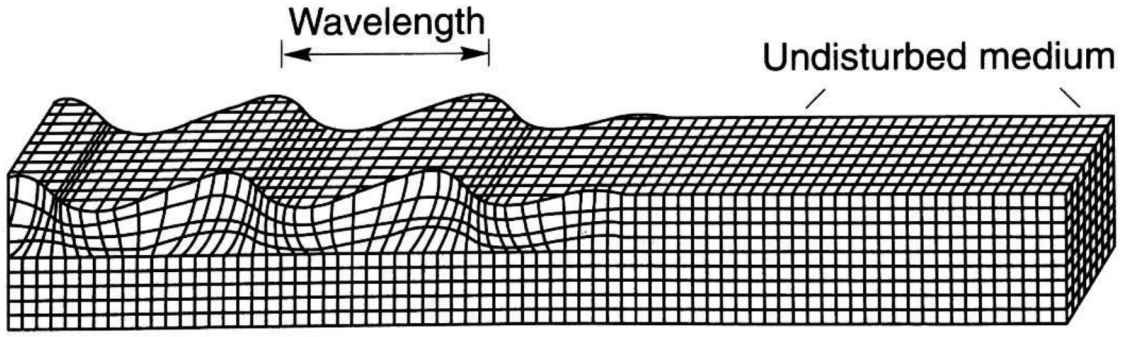

Figure 2.6: Motion of medium during Love wave propagation. Reprinted with permission from [20].

2.2.2 Damping

Vibrational energy moving as a wave through a medium will lose energy as it propagates, in part by material damping and in part by geometrical attenuation.

Geometrical attenuation occurs when the energy spreads over a larger space as it travels from the source. Body waves spread in all directions in a half space and thus in an overall larger space compared to the surface waves. The decay factor of the vibrational energy will then differ, as can be seen in table 2.1 and was determined by Horace Lamb. For example for a surface wave emitted from a line source propagating through a perfectly elastic material, the wave would be able to travel infinitely long without a change in amplitude. Since the geometrical attenuation is much greater for body waves than surface waves, the surface wave is dominating further away from the source. It is often the most relevant wave type affecting building. For an elastic material the geometrical attenuation from oscillating point or line source is determined by Lamb's equation:

$$\hat{v} = \hat{v}_1\left(\frac{r_1}{r}\right)^m, \tag{2.5}$$

where $\hat{v}_1$ is the top vibration amplitude at distance $\hat{r}_1$ and $\hat{v}$ is the top vibrational amplitude at a distance r from the source. The constant m is dependent on the

type of wave, propagation and wave and is found in table 2.1.

Propagation	Source type	Wave type	m	Decay factor
Along surface	Point source	Body wave	2	$1/r^2$
Along surface	Point source	Surface wave	0.5	$1/\sqrt{r}$
In half space	Point source	Body wave	1	1/r
Along surface	Line source	Body wave	1	1/r
Along surface	Line source	Surface wave	0	No decay
In half space	Line source	Body wave	0.5	$1/\sqrt{r}$

Table 2.1: The constant m in Lamb's equation and the decay factor depending on propagation, source and wave type.

Material damping occurs as there are inner frictions in the material trough which the wave is propagating. Lamb's equation was extended by Bornitz to include this and looks as follows:

$$\hat{v} = \hat{v}_1 \left(\frac{r_1}{r}\right)^m e^{[-\alpha(r-r_1)]}, \tag{2.6}$$

where the added exponential term represents the material damping. The constant α is called the damping factor and varies with different materials and vibration frequency according to:

$$\alpha = \frac{2\pi f \cdot \xi}{c}, \tag{2.7}$$

where f is the frequency of vibration, ξ is the damping ratio of the geo-material and c is the propagation speed. That is the material damping increases with propagation speed (i.e. the stiffness of the material) and frequency. It is thus greater in looser soil compared to firm soil. Another important property is that higher frequencies are much more attenuated than lower frequencies. It is therefor possible for low frequency vibrations to spread over large distances in firm soil. Table 2.2 show typical values of the damping factor α for different soils with a specific frequency, determined by Woods and Jedele (1985).

Coefficient α (m^{-1})		Material description
5 Hz	50 Hz	
0.01-0.03	0.1-0.3	Soft soils (shovel can easily penetrate): Organic soils, loose to semi-stiff clay, very loose sand.
0.003-0.01	0.03-0.1	Competent soils (can be penetrated by shovel): stiff clay and loose to mid stiff cohesionless soil.
0.0003-0.003	0.003-0.03	Hard soils (too hard for shovel): very stiff clay, cohesionless soil and relatively stiff weathered rock materials.
<0.0003	<0.003	Bedrock

Table 2.2: Values of material damping coefficient α for four different soil materials.

2.2.3 Geology

The softer material encountered in the earth crust is called soil. It is usually composed of solid grains in-between which are pores containing air and/or water. There are two types of soils: mineral and organic. Organic soils consists of at least 20% organic material and a few examples are peat and muck. Mineral soils consists of less organic material and some examples are sand and gravel. Soils can be categorized into cohesive and non-cohesive, sand and gravel also being an example of the latter one. Non-cohesive soils are being bound together by the particle friction. For the cohesive soil the mechanisms binding the particles together are inter-molecular forces as well as friction. Clay and silt are examples of cohesive soils. In practice it might not be as simple as these categorizations. What one instead might encounter are mixes of material types and with this follows a wide range of structural behaviours. If the material stiffness increases with depth it can cause dispersion. A saturated soil can become relatively soft and susceptible to deformation while a dry soil are typically more stiff. According to ISO 14837 [19] viscous damping at high frequencies can be produced in water saturated porous soils. Ground materials are however generally stiffer under compression load, compare to shearing load. Table 2.3 presents some ground material properties, based on [14]. c_p and c_s are wave propagation speed (m/s) of compression and shear wave. ν is the Poisson's ratio, ρ is the density (Mg/m^3) and G_{max} is the shear modulus (MN/m^2).

Material:	c_p **&** c_s**:**	ν**:**	ρ**:**	G_{max}**:**
Loose sand	1450-1550 & 100-250	0.48-0.50	1.5-1.8	15-110
Medium-firm sand	1500-1750 & 200-350	0.47-0.49	1.7-2.1	70-250
Stiff sand	1700-2000 & 350-700	0.45-0.48	1.9-2.2	230-1000
Loose clay	1450-1550 & 80-180	0.47-0.50	1.6-2.0	10-65
Medium-firm clay	1500-1700 & 180-300	0.47-0.50	1.7-2.1	55-190
Stiff clay	1600-1900 & 300-500	0.47-0.50	1.8-2.3	160-450
Sandstone	1400-4000 & 800-2000	0.25-0.35	2.0-2.4	1300-9500
Limestone	2100-6000 & 1200-3000	0.25-0.35	1.8-2.5	2600-20000
Gneiss	3500-7000 & 2000-3500	0.25-0.35	2.2-2.6	8500-32000

Table 2.3: Properties of ground material. Values acquired from [14].

As the wave travels through soil the properties of the soil will have an effect on the wave. Many factors will influence the behaviour of the ground material, for example a change of stiffness over depth can cause dispersion, or the saturation of water will affect the speed of the wave. Two typical ground types on the west coast of Sweden are *glacial clay* and *post glacial fine sand*.

Sediments that are deposited in connection with melting glaciers are called glacial and sediments later deposited are called post glacial, with some of the post glacial sediments still being deposited today. Such a ground type is the glacial clay, being a soil consisting of fine-grained clay particles that was deposited during the last icecaps melting [24]. It can sporadically carry the larger stone and sand particles.

The post glacial fine sand consists of larger particles than the clay. It is therefor easier to dig through the sand as it also has larger space between the particles and are not as good carrying water.

2.2.4 Ground vibration boom

The ground vibration boom is a phenomenon similar to the airborne sonic boom, being a kind of shock wave that is generated at the wave front. This can happen in either one of two ways. The first one is if the train speed is similar to the velocity of the surface running Rayleigh wave's propagation speed in the near subground, referred to as critical wave speed [21]. The second on is if the train speed is similar to the minimum of the phase velocity bending wave in the rail, referred to as critical track speed [21]. If this happens the wave amplitudes starts interfering with each other and the ground vibration levels can have a dramatic increase. The wave front then propagates in the shape of a semi-cone from the train front. The speed of the Rayleigh wave is relatively low for loose ground materials, see table 2.3. The water saturation is important to have in mind as well during a site characterisation. If the characterisation is done during a dry period the soil might seem firm but with rain it can become very loose. The phenomenon was observed near Ledsgård at the Swedish west coast where very loose clay (muck) made up the ground. Here the Rayleigh propagation speed could go down to 45 m/s meaning a train speed of around 162 km/h was sufficient to generate ground vibration booms, resulting in a tenfold increase of the ground vibration levels.

The critical track speed of a rail can be calculated via:

$$c_{min} = \left(\frac{4\alpha EI}{m_0^2}\right)^{1/4}, \tag{2.8}$$

where E is the Young's modulus, I the rail's moment of inertia, m_0 the mass per unit length and α is a proportionality coefficient modelling the elastic ground, based of the equivalent Winkler elastic foundation [21]. When the velocity of a train approaches the critical track speed, deformations in the rail starts to form.

2.2.5 Refraction and reflection

As a wave encounters an impedance change, e.g. when it reaches the boundary of another material or soil layer, with another density and/or stiffness, one of two things happens. Refraction, being the change in direction of the wave as a result of the change of speed that the wave experiences entering the new material, or reflection where the wave is being reflected back instead of entering the new material. Waves refract and reflect different depending on material and velocity and occurs only during impedance changes making the phenomenon mainly appearing in layered materials (soils).

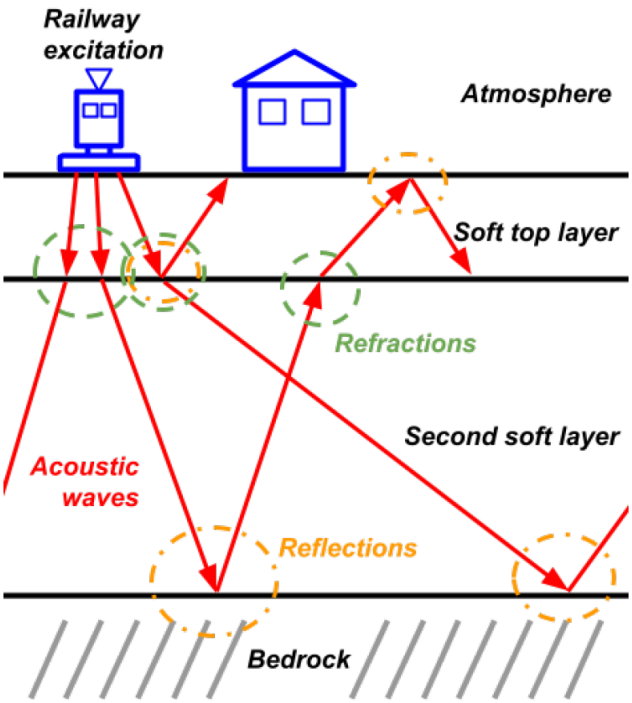

Figure 2.7: Reflection and refraction of ground vibrations. Reprinted with permission from [14].

2.2.6 Ground resonances

A source such as a railway will emit vibrations over a range of frequencies. If a ground layers eigenfrequency corresponds to the frequency of the source then resonances will occur. Each resonance will then greatly increase the amplitude of the vibration.

For a homogeneous soil the n^{th} eigenfrequency f_n can be estimated by (Roësset, 1977):

$$f_n = \frac{(2n+1) \cdot c_s}{4H}, \tag{2.9}$$

where $n = 0, 1, 2, ...,$ or $n \in \mathbb{W}$ is the order of the eigenfrequency and H is the depth of the ground layer. Each excited eigenfrequency will develop a standing wave, as is presented in figure 2.8. The largest amplitude amplification occur at the lowest eigenfrequency, i.e. the fundamental frequency of the soil layer, and attenuates as the order of eigenfrequency increases, as seen in the figure. As such it is often only the fundamental frequency that is of interest for engineering purposes. Equation 2.9 implies that a deep soil layer of loose homogeneous soil will amplify low frequent signals while a thin layer of stiff soil amplify high frequent signals.

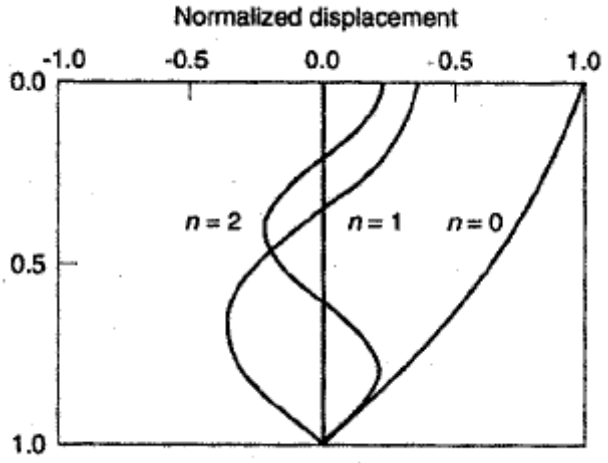

Figure 2.8: Mode shapes/deformation pattern of standing waves for different eigenfrequency orders in a homogeneous soil layer. Reprinted with permission from [14].

2.3 Receiver

The final phase of the vibration is when it reaches a receiving element. This could be many things but the main ones of interest are the human response to vibrations as well as building responses.

The impact of vibrations on humans comes in a wide range depending on the strength and frequency of the signal. Weak vibrations might not be noticed at all by humans, being below the threshold of perception, meanwhile ground-borne noise almost always being noticeable. For vibrations above the threshold of perception humans can feel them either via the entire body, with their hands or when standing/sitting/lying. The standard ISO 2631 [26] shows how to assess human exposure to vibrations and that the sensitivity of it usually is the highest from 8 to 80 Hz.

As a ground-borne vibration travels into a building's structure there is a risk for it to amplify. An example of when such a risk is present is when the floor spans are long. To explain the effects a building's frequency response function can be used. Although damage to buildings from ground-borne vibrations can be a concern it is rarely the case [25]. The strength of vibrations typically reported in cases of minor cosmetic damage are larger than 5 mm/s (maximum values), meanwhile vibrations caused by trains are generally in the order 0.1 to 0.6 mm/s (average values).

2.3.1 Structure borne sound and vibrations on buildings

When determining measures for reaching the requirements for buildings in terms of structure borne sound and vibrations it is often done through a *functional requirement*. This is because the energy that is transmitted into the building is highly dependant on the buildings frequency response, where it usually comes down to

the frequency response of the foundation. The attenuation of structure borne sound and vibrations is effectively determined by the frequency response of the foundation.

The foundation, or any other element of a building for that matter, will act as a mass-spring system, through which the vibrational energy has to pass. In short a mass-spring system is a mechanical system consisting of a mass attached to a spring. If the mass is put into motion it will start to oscillate, independent of gravity or the starting displacement of the mass. By isolating the system it will move with its natural frequency, depending on the weight of the mass and the stiffness of the spring. When energy in the ground of certain frequencies enters the system the output will be determined by the frequency response. Frequencies close to that of the eigenfrequencies of the mass-spring system defined by the foundation will be increased while others will be decreased. In practice it comes down to decreasing the first eigenfrequency. Generally it becomes more expensive the lower the eigenfrequency and the attenuation becomes sufficient quite fast after you pass the first eigenfrequency.

2.4 Regression analysis

Regression analysis is a statistical tool used to estimate the relationship between independent variable(s) and dependent variable(s) (e.g. an outcome). The dependent variable usually varies with the independent variable(s) and the regression analysis tells us how much each independent variable matters towards a change in the dependent variable(s). Linear regression is the most regular version which is used to fit a line (or linear combination of more complexity) as close as possible to the available data, following a specific mathematical formula. An example of this can be seen in figure 2.9.

The blue line in figure 2.9 was acquired using the method of least squares (LSM). It gives the line which minimizes the sum of all squared differences between each data point and that line.

An example of computing a line using LSM can be done as follows. Suppose it is desired to find the line that shows the behavior of the red dots in figure 2.9. First a mathematical criterion needs to be set for the line, in this case it seems to be linear, following the equation

$$y = kx + m. \tag{2.10}$$

For example the red dots could be the noise that a car emits with the y-axis being the sound pressure level and the x-axis being the velocity of the car. The x and y in equation 2.10 is then known, where LSM will solve it for the unknown parameters k and m. k would in this case relate the emitted noise to the velocity of the car. To solve this the problem needs to be presented as a matrix system. Say there data available consist of n points. The matrix system then looks like:

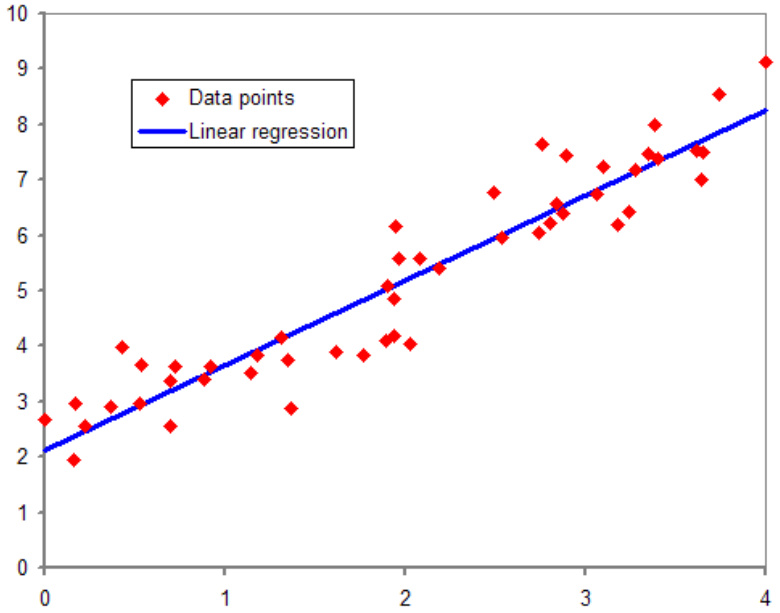

Figure 2.9: Example of linear regression. The red dots represent collected data points and the blue line represents the fitted line acquired via linear regression. Reprinted with permission from [3].

$$\begin{bmatrix} x_1 & 1 \\ x_2 & 1 \\ \vdots & \vdots \\ x_n & 1 \end{bmatrix} \cdot \begin{bmatrix} k \\ m \end{bmatrix} = \begin{bmatrix} y_1 \\ 1_2 \\ \vdots \\ y_n \end{bmatrix} \tag{2.11}$$

and has the shape $A \cdot b = y$. This is a matrix system that can be algebraically solved for b.

$$A \cdot b = y \tag{2.12}$$

To solve for b the A can be made into the identity matrix by multiplying it with its inverse A^{-1}. This can however at the current state not be done as A no a quadratic matrix. First it needs to be multiplied with its transpose A',

$$(A'A) \cdot b = (A'y) \tag{2.13}$$

The matrix next to b is now quadratic and the final step can be applied by multiplying both sides with $(A'A)^{-1}$:

$$b = (A'A)^{-1}(A'y) \tag{2.14}$$

The vector b now contains the values for k and m for the fitted line is now calculated.

3

Model

This section will explain the HS2 model. As not the entire model is within the scope of this project some parts of it won't be explained en further detail. Figure 3.1 shows a flow chart of the HS2 model, the green color highlighting the steps that are within the scope. This encompasses vibrations in the ground at a distance from a surface running train. The concept of the model is basing the prediction on a reference passage and then correct that lithology spectrum for a number of parameters where the reference train might differ from the predicted train. The reference train is chosen by choosing one out of four lithologies. The steps of the HS2 model included in the implementation and within the scope of this thesis are:

- Lithology
- Mass
- Track-train dimensions and speed
- Track system
- Distance

A fundamental explanation of how they affect the ground vibration levels can be seen in the theory section 2. Tunnel sections and building responses are part of the HS2 model but will not be covered (although briefly explained in section 2.3).

1. Lithology and source terms
The first step of the HS2 model is identifying the lithology around the track formation and match it with the proper reference source spectrum of the model. The model has 4 source terms, one for each generic classification on lithology: sand, clay, mix of sand and clay and lastly chalk. The source terms spectrums are shown in figure 3.2 and are measured on good quality ballast tracks in UK and France [5]. They are defined by the vibration velocity level 10 meters away from the track, presented as the RMS in dB (reference value $10^{-}9$ m/s). The signal covers the whole passage period, presented in third octave bands in a range of 6.3 to 250 Hz (not all of them go all the way up to 250 Hz). As seen in figure 3.2 the Eurostar train is used for all surface source terms except for clay where the CL322 train is used.

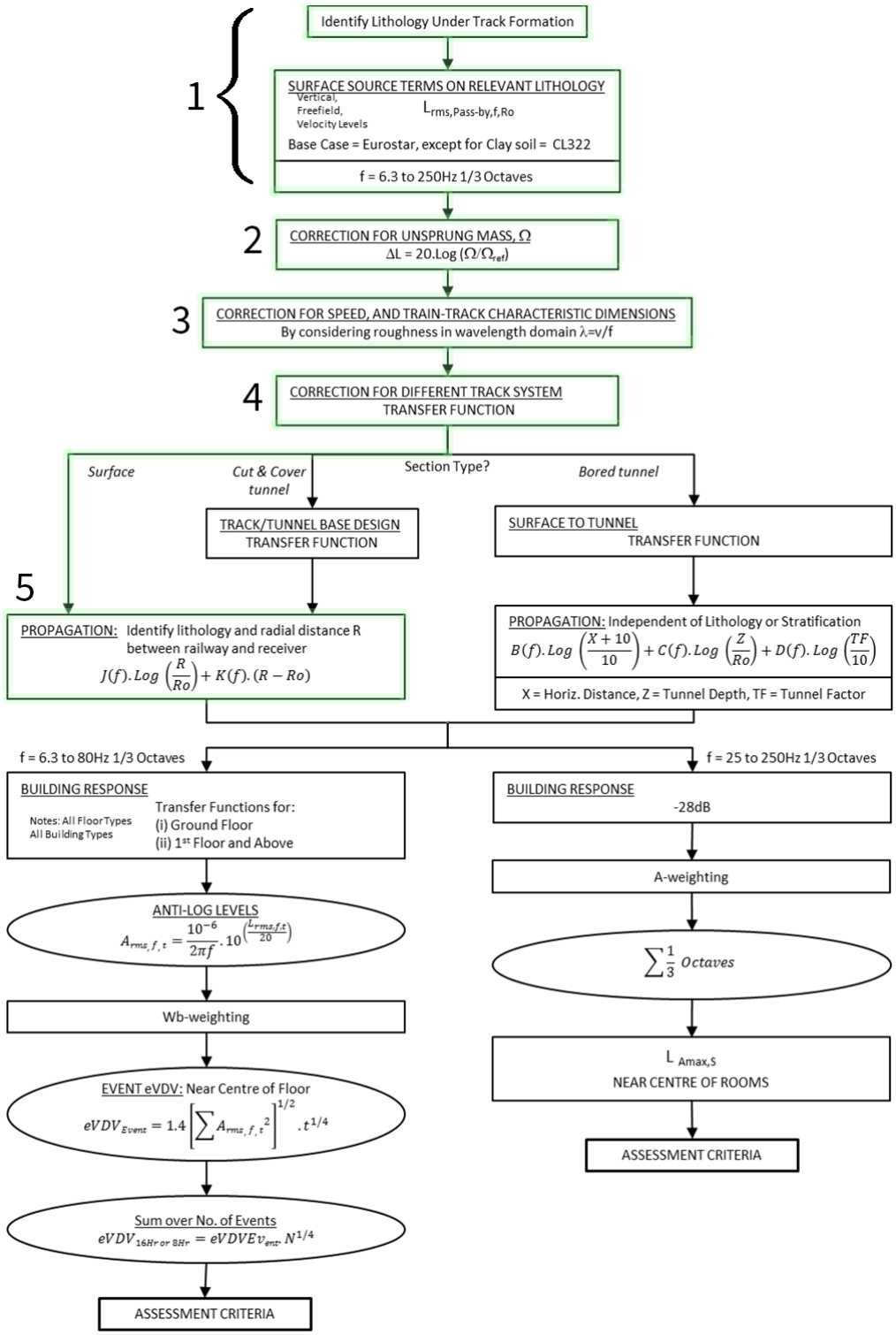

Figure 3.1: Flow chart of the HS2 model. The highlighted path in green is the scope of this project and the implementations in Matlab. Picture adapted from [5].

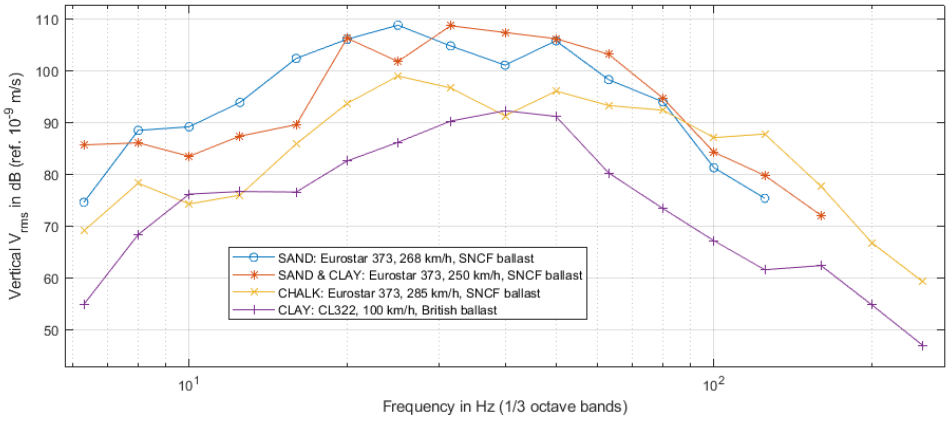

Figure 3.2: The spectra of the HS2 models source terms. Each spectrum refers to a specific lithology, track type, train type and speed.

2. Unsprung mass

The next step is to correct for difference in mass between the reference train used for the source terms and the predicted train. This is done by adding a mass correction factor, being the logarithm of the ratio between the actual unsprung mass of a train car and the reference mass, which is 1000 kg. The unsprung mass is defined as the average unsprung mass per wheel axle, i.e. the mass of the wheels, axles and any equipment mounted on the axles such as wheel bearings, hubs, partial weight of springs, driveshafts and suspension links. Excluded is all the mass supported by the suspension, e.g. the body of the train and components attached to it.
The unsprung mass correction factor, denoted ΔL, is frequency independent and is defined by the equation:

$$\Delta L = 20 \cdot \log_{10}\left(\frac{\Omega}{\Omega_{ref}}\right). \tag{3.1}$$

ΔL is then added to the chosen source spectrum.

3. Speed and Train-track characteristic dimensions

Here corrections for the difference between the reference train and the predicted train in dimensions of the train and track as well as for the train speed are done. The dimensions are used to define the parametric excitation that is being caused by the dynamic interaction between the rail and the wheels and they are defined in ISO 14837 [19] and can be seen in figure 3.3.

The model step is designing a function termed the effective roughness R_{eff} (roughness amplitude over wavelength). This is done for both the reference train and the predicted train where the difference will be the result of this step. R_{eff} is initialized by a derivation of a generic roughness profile that is representative of good quality ballast track [4], for a wavelength range of 0.01 to 25 m. The spectrum stems from measurements from a Crossrail noise and vibration evaluation [7] and a corrugation analysis trolley at Steventon, England [9]. This spectra will then be modified by

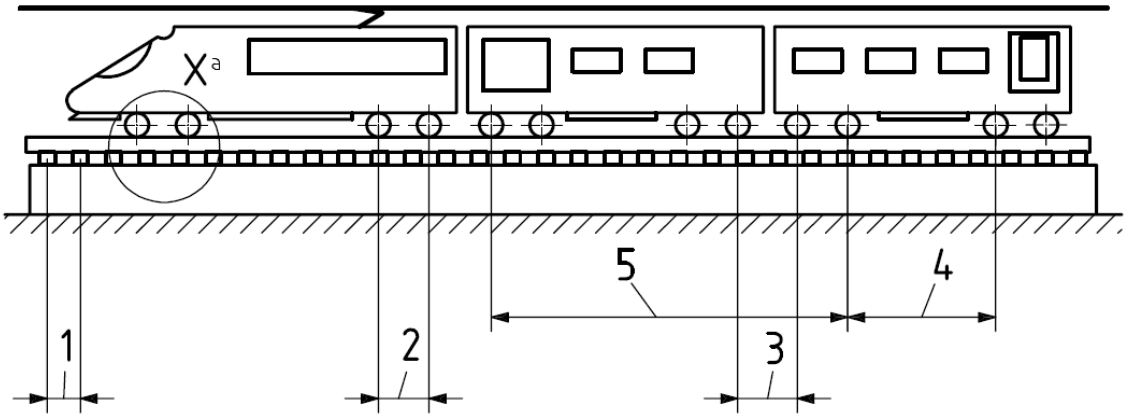

Figure 3.3: Axle dimensions for the model. Dim. 1 is the sleeper distance and dim. 2 - 5 are train related regarding the wheel setup. Reprinted with permission from [19].

parabolic functions defined by the dimensions of the trains. The effective roughness R_{eff}, the generic roughness spectra and the parabolic functions can be seen in figure 3.4 where the symmetry line of the parabolic functions is at the wavelength corresponding to the dimension value. The parabolic functions are defined by

$$L_K(\lambda) = R(\delta_K) + A - \left(\frac{\log\lambda - \log\delta_K}{B}\right)^2 \tag{3.2}$$

where L_K is the parabolic function, being the contribution in vibration level, of the K^{th} sleeper or axle spacing. λ is the wavelength in metres and δ_K is the K^{th} sleeper or axle dimension. $R(\delta_K)$ is the value of the generic roughness spectrum at the wavelength of the symmetry line for the K^{th} sleeper or axle spacing. A and B are constants for the amplitude and width of the parabolic functions and can be manually tuned to make the prediction better fit the measurement data if desired. For example, in figure 3.4 the sleeper spacing, corresponding to dim 1 (orange) has its symmetry line at the wavelength $\lambda = 0.55$ m as that is the sleeper distance. L_2, L_3, L_4 and L_5 corresponds to axle dimensions 2, 3, 4 and 5.

The calculated L_K functions and the generic roughness spectrum are then superimposed and the final train-specific effective roughness R_{eff} is obtained. This process is done for the reference train and the prediction train. The superposition is following the equation

$$R_{\text{eff}}(\lambda) = 10 \cdot \log\left(10^{R(\lambda)/10} + \sum_K 10^{L_K(\lambda)/10}\right) \tag{3.3}$$

The resulting effective roughness R_{eff}, the generic roughness spectra and the parabolic functions for an example train can be seen in figure 3.4.

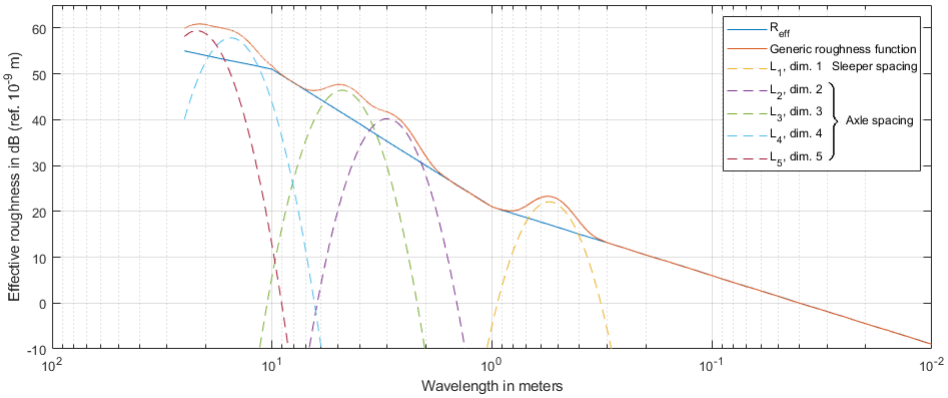

Figure 3.4: The superimposed R_{eff}, the generic roughness curve as well as the parabolic functions, L_K's, which represents the effects of the track-train dimensions according to figure 3.3.

The roughness spectra will now be related to the speed of the train. Using the relationship $\lambda = \frac{v}{f}$, where v is the speed of the train, the roughness spectrum can be plotted over frequency instead of wavelength. Doing this for the reference train and prediction train, the final correction factor for train-track dimensions and speed is calculated by taking the difference between the reference train spectrum and prediction spectrum of each one third octave band, ΔR_{eff}. This is then added to the reference spectrum.

4. Track system

This step accounts for the effects of the difference in track systems between the reference train and proposed train, ΔIL. Different track systems leads to different insertion losses which in the model are defined as the change in vibration levels 10 m from the nearest rail when replacing a track with another.

The HS2 model has insertion loss data defined for 3 track systems [6]. They are;

- SNCF Ballast - standard ballast of the French National Railway Company
- BR Ballast - standard ballast of the British Rail Company
- Base case track

where the base case track is stated to be a resilient slab track optimised for vibration isolation and track stiffness similar to ballast track [6] [4]. The track systems are presented in figure 3.5. As can be seen the insertion loss is negligible at lower frequencies, negative for center frequencies at a range depending on the ballast type, and increasing a lot for higher frequencies.

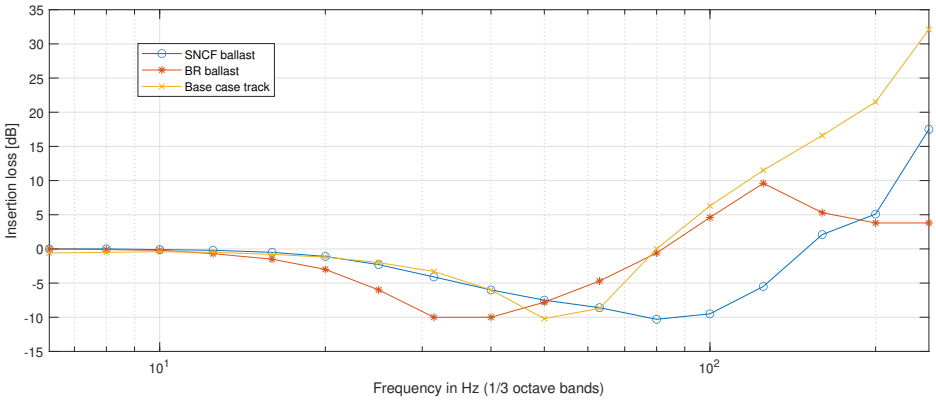

Figure 3.5: Insertion loss spectrums for the HS2 source terms.

5. Propagation

This step corrects for propagation at a specified distance from the nearest rail. It accounts for geometrical attenuation and material damping for the chosen lithology. This propagation model is based on vibration analysis of measurements from a variety of trains in Germany, France and the UK. It follows the equation

$$P_{corr} = J(f) \log \frac{R}{10} + K(f)(R - 10) \tag{3.4}$$

where $J(f)$ and $K(f)$ are lithology specific propagation coefficients in third octave bands and can be seen in Table 7 of Annex D1 in [4]. These terms can be calculated using regression analysis as explained in section 2.4. The equation 3.4 is designed to fit the reference source terms which are measured at 10 m distance. Set $R = 10$ m and the correction P_{corr} becomes 0 which is desired. It then increases with $R < 10$ and decreases when $R > 10$. When the propagation correction is calculated it is added to the source spectrum.

Now a ground vibration level at a certain distance from the rail is acquired. Further steps of the model are outside the scope of this thesis but will be briefly explained in the following step.

6. Further steps

The next step introduces building transfer functions which is used to get the ground vibration level translated into excited vibration levels at a specific floor within a building.

It then calculates Anti-log levels. This step also includes an integration in the frequency domain to convert the velocity levels into acceleration. This is done by multiplying with a factor $2\pi f$. The Anti-log levels are calculated by:

$$A_{rms,f,t} = 2\pi f \cdot 10^{-6}\Big(\frac{L_{rms,f,t}}{20}\Big) \tag{3.5}$$

The next step is applying an appropriate weighting filter, depending on the goal of the prediction. Now the estimated Vibration Dose Value (eVDV) can be calculated. It is calculated at the centre of a floor span for a specific train passage, defined by the equation:

$$eVDV_{event} = 1.4\Big[\sum A^2_{rms,f,t}\Big]^{1/2} t^{1/4}, \tag{3.6}$$

where t is the time of the train passage and $A_{rms,f,t}$ is the acceleration close to the centre of the floor span. The last calculating step is to sum up the number of passages over an 8 or 16 hour time span, following the equation:

$$eVDV_{16Hror8Hr} = eVDV_{event} N^{1/4}, \tag{3.7}$$

where N is the amount of passages occurring in the chosen time span. With the prediction finished it can now be determined if measures to reduce the vibrations should be taken or not.

4
Method

This section covers the methodology of the thesis, starting with explaining what is needed in order to fulfill the goals of the thesis. It follows with a section about the measurement sites, then the actual procedure during the measurements. After that is the evaluation process section, explaining how the model data and measurement data are to be evaluated and what tools are to be used. Next is a section of the uncertainties of some model parameters, and analysing their impact. Last is a section of the implementation of an additional lithology to the model.

The goal of the thesis is to evaluate the HS2 model in Sweden, under Swedish circumstances. For this purpose two measurement sessions were made at the west coast of Sweden. To be able to properly compare the measured data with the model it is important to gather as many of the HS2-parameters during the measurement as possible. For a detailed information about the model see section 3, but in short the main parameters are:

- lithology under track formation
- unsprung train car mass
- train and track dimensions
- train speed
- track system
- distance between measurement point and nearest rail

In general it is likely to be limitations of the data collected. Extensive geological data of a specific measurement site is not likely to be available. This is important when analysing the measured data, however picking the right lithology in the case of the HS2 model should not be an issue even without extensive geological data. Unsprung mass of the train cars, information about the track system as well as train wheel axle dimensions can also be troublesome to acquire. During the measurements as much data as possible should be recorded and after that specific train or track data can be sought for from external sources such as Trafikverket [16], Transportstyrelsen [17] and train developer/owners. The documentation of these parameters and more are further explained in section 4.2 down below.

With the measurements done, parameter data collected and with the model at hand an evaluation process can be started. This process is explained in section 4.3.

During the project two sites were measured at, both on the west coast of Sweden,

south of Gothenburg. One close to Åsa train station in Åsa and one in Lindhov. The soil there is loose and has as such good potential for large vibrations. It can in that way act as a stress test for the model.

During the measurements a set of parameters had to be documented. This set consisted of mainly the different train types, speeds, distances and soil types. To be able to carry out measurements near the railway approval of Trafikverket was applied for. To ensure reliable data Trafikverket also delivered information about train types and passages. The two measurement sites were chosen based on Geomap [11] (or "Geokartan" in Swedish), provided by SGU, the Geological Survey of Sweden. The Geomap is a map of Sweden with geology data including the soil type, bedrock depth and more. It is constantly updated as Sweden is being charted and covers a lot of the country, however the data is sample derivated and should be taken as approximations and as such as a potential source of uncertainty. The two measurements sites were chosen with different soil types and the measurements were performed in the same way on both of them.

4.1 Measurement sites

4.1.1 Åsa

The first location is a couple of hundred meters north of Åsa train station in Åsa. The measurement was performed 16th of May 2022. Figure 4.1 shows a geological map from Geomap with markings of the measurement points. MP1 is at 10 m from the closest rail, MP2 at 20 m and MP3 at 40 m. The measurement points should preferably be aligned perpendicular from the rail, however as requested by the land owners, to not disturb the soil as much, they were chosen along ditches at the site. The soil at Åsa according to Geomap [11] is glacial clay, a lithology further explained in 2.2.3. The bedrock depth is at 10-20 meter according to Geomap and the experience of digging the holes for the geophones was rather troublesome as it was quite rich with rocks and pebbles.

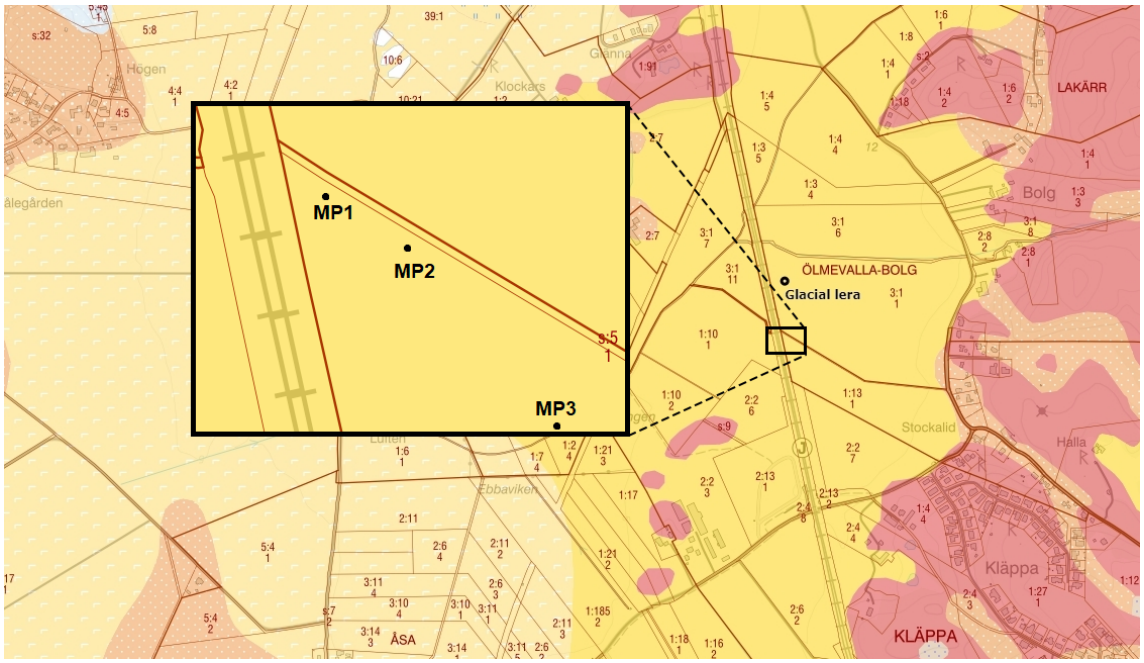

Figure 4.1: Åsa station as seen on Geomap.

Table 4.2 shows data from the passages. For each recorded passage it shows the train and model, if it stopped at the nearby Åsa train station, the recorded speed and at which track of the double track railway the train went on. Train number and vehicle ID number were supplied by Trafikverket. The train model could be achieved with the vehicle ID using Transportstyrelsens vehicle register [17]. The vehicle register also included some of the wheel dimensions needed for the HS2 model, according to ISO 14837 [19]. Wheel dimensions were also acquired by direct contact with transportyrelsen and the data can be seen in table 4.1. There is however still uncertainty in the data. Transportstyrelsen didn't have information on all the model variations and also suggested confirming the data with the vehicle owner to confirm it. Another factor is that trains usually consists of different car types which have different wheel setup and weight. A regular passenger train usually consists of a locomotive car, passenger cars and in the end a caboose, where all 3 car types have different dimensions. The dimensions used, being the ones acquired from Transportstyrelsen, can be seen in table 4.1.

		Train dim. according to SS14837			
Tåg	**Modell**	**2**	**3**	**4**	**5**
Öresundståg	X31K	2.7	4.125	16.3	25.825
SJ	X55	2.7	4.9	16.3	26.6
Regina	X61	2.7	4.8	16.3	26.5

Table 4.1: Train dimensions according to ISO 14837 for each respective train type.

In total there were 16 passages, resulting in 48 recorded transients (3 per passage,

	Time	Train	Model	Stopping	Speed [km/h]	Track
1	13:52	SJ	X55/B	No	198	Near
2	14:07	Öresundståg	X32K/M43	No	180	Near
3	14:15	SJ	X55/B	No	198	Distant
4	14:27	Öresundståg	X31K/M43	No	178	Distant
5	14:39	Öresundståg	X31K/M43	Yes	70	Near
6	15:07	Öresundståg	X31K/M43	No	178	Distant
7	15:10	Öresundståg	X31K/M43	No	146	Near
8	15:21	Regina	X61/A	Yes	96	Distant
9	15:37	Regina	X61/A	Yes	78	Near
10	15:50	Öresundståg	X31/OTU-CFT-A	No	178	Distant
11	15:51	SJ	X55/A	No	196	Near
12	16:08	Öresundståg	X31K/M43	No	170	Near
13	16:23	Regina	X61/A	Yes	94	Distant
14	16:35	SJ	X55/B	No	194	Distant
15	16:39	Regina	X61/A	Yes	76	Near
16	16:51	Öresundståg	X31K/ET	No	176	Distant

Table 4.2: Model relevant data from train passages at Åsa station.

one for each geophone). Out of the 16, five where of trains stopping at the station (marked orange in the table). These are to be analysed as a separate group, as the scenario is not what the HS2 model is directed at and the speeds are lower and not well defined as they are changing drastically during the train passage. It is however possible that acceleration can give rise to large vibrations and should as such be analyzed as well. The 11 regular measurements recorded train speeds between 146-198 km/h (mostly 178-198 km/h). The 5 slower trains had a speed of 70-96 km/h. Most of the trains are Öresundståg, with some SJ and Regina trains. The Regina trains were also the only ones stopping at the station. The transient reports can be seen in Appendix A.

4.1.2 Lindhov

The second location is in Lindhov, see figure 4.2 for a geological map with markings of the measurement points. The measurement was performed 20th of May 2022. The soil at Lindhov according to Geomap [11] is post glacial fine sand, further explained in 2.2.3. The bedrock is approximated at 5-10 meters depth.

The train passages data are presented in table 4.3. In addition to the presented parameters in the Åsa table 4.2, it also shows the corresponding train type for each passing train. RST stands for "resandetåg" or passenger train, GT stands for "godståg" or freight train and TJT standing for "tjänstetåg" or work/engineering train. In total 20 trains passed, resulting in 60 recorded transients over the 3 geophones. The freight train of the 14th passage, at 16:33 was long enough to be measured as 2 transients of the geophones, as can be seen in the table. 9 of the measurements had data missing in the recordings (marked red in the table), e.g. speed or vibrations

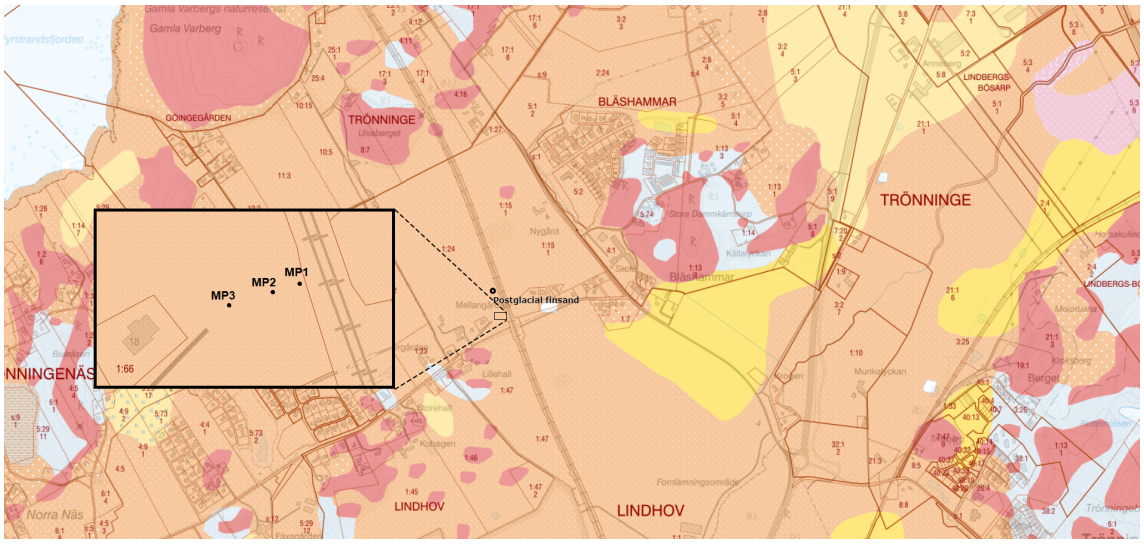

Figure 4.2: Lindhov station as seen on Geomap.

not being recorded. All of these were discarded but their data and what data is missing can be seen in Appendix A. Of the remaining 11 measurements 3 of them are from none passenger trains, which will be evaluated as a separated group. This results in 8 passages to be used as a main data set to evaluate the HS2 model.

4.2 Measurements procedure

The vibrations were measured using three geophones buried in the ground at fixed distances to the closest rail, at 10, 20 and 40 meters. As it is a double track system then trains are traveling on both tracks resulting in distances of approximately 13, 23 and 43 meters being measured as well. A speed radar was simultaneously measuring the train speeds. All of the measurement devices were connected to an INFRA Master unit which controlled the measurement tools, handled and logged all data and live sent it to the Infranet server. Following is an equipment list as well as a description of how the measurements were made practically.

Equipment list for measurements

- INFRA V12 triaxial geophone
- INFRA Master
- INFRA X20SR Speed Radar mounted on a tripod

The INFRA v12 triaxial geophones is the device measuring the ground vibrations. It converts the measured ground movement (velocity) into voltage which is sent to the Infra Master unit. The geophone has a wide range of standards to pick depending on what should be measured, e.g. vibrations from blasting or for human comfort in buildings. A list of all the standards can be found in the manual for the V12, see [12]. The standard used was S54, measuring unweighted velocity in a level range of 5000 µm/s and frequency range 5-500 Hz. As the HS2 model uses the unweighted velocity levels in a range of 6.3 to 250 Hz it covers the frequency range of the model.

	Tid	Tåg	Modell	Tågslag	Speed [km/h]	Track
1	14:50	Öresundståg	X31K/M43	RST	80	Distant
2	14:53	Öresundståg	X31/OTU-CFD-A	RST	108	Near
3	15:07	Locomotive	-	TJT	102	-
4	15:11	Regina	X61/A	RST	76	Near
5	15:15	Freight train	RM/-	GT	70	Near
6	15:16	Öresundståg	X31/OTU-CFD-A	RST	174	Distant
7	15:22	Freight train	-	GT	64	Near
8	15:42	Öresundståg	X31K/M43	RST	120	Near
9	15:49	Regina	X61/A	RST	118	Distant
10	16:00	SJ	X55/A	RST	N/A	Distant
11	16:10	Regina	X61/A	RST	130	Near
12	16:22	Öresundståg	X31K/A	RST	164	Distant
13	16:26	SJ	X55/A	RST	126	Near
14	16:33	Freight train	RM/-	GT	N/A	Near
↑	16:34			GT	N/A	⌢
15	16:49	Regina	X61/A	RST	N/A	Distant
16	16:54	Öresundståg	X31K/M43	RST	N/A	Near
17	17:05	Regina	X61/A	RST	N/A	Distant
18	17:10	Öresundståg	X31K/ET	RST	N/A	Near
19	17:17	Öresundståg	X31K/M43	RST	N/A	Distant
20	17:35	Regina	X61/A	RST	N/A	Distant

Table 4.3: Data from the Lindhov passages.

The V12 has 3 further parameters required to be set; interval time, threshold and recording time. The interval time sets how often the maximum velocity value is stored and in the project the default value of 2 minutes was used. The threshold determines at what vibration level data should start being recorded. For the setup used in the project only the geophone closest to the rail could trigger an event and start a recording. This was to reduce the risk of any false sources (e.g. cars, tractors etc.) triggering measurements. The last parameter was the recording time. It sets the length of the recording of any transient file, in this case 1 min.

The geophones measures horizontally (lateral and transversal respectively) as well as vertical. Note that the model only output vertical vibrations which is what will be compared but that the horizontal data can be important to validate the result as a whole as well as being used for analysing the presence of the different wave types. The geophones operate while being underground and thus required digging holes, where the depth from the top of the geophone to the surface should exceed approximately three times the height of the geophone (around 40 cm), according to NT ACOU 082 [8]. An example of a hole at Åsa station can be seen in figure 4.3. The hole dimension had to be around 40 cm x 30 cm to fit the geophone with the cable, as well as a spirit level. According to the manual [12] in order to get correct measuring results, the mounting angle must not exceed a 5 angle relative to the reference plane. The geophone unit was positioned so that the bubble in the spirit level stayed between the lines indicating a degree of less than two from the horizontal plane. On the geophone were arrows showing the direction of the unit, i.e. which side should point perpendicular and parallel to the rail respectively. It was covered in a plastic bag for a basic dirt protection and the position and level were secured with pushing a bolt through the unit into the ground followed by carefully refilling the hole.

The INFRA X20SR Speed Radar measures the speed of the passing trains [13]. The position and angle of the radar is important for reliable results. For rail vehicle measurements the radar should be positioned 5-10 meters from the rail and have the radar face sideways so that its center line of direction hits the rail 40-70 meters away. Depending on the actual distances a correction factor needs to be added to the measured speeds. The correction factors can be seen in table 4.4. A schematic picture of the parameters in the table can be seen in figure 4.4 to the right, as well as the actual speed radar setup to the left. A rule of thumb for the setup to secure a measurement error less than 3.5% due to radar placement is to assure that 70m $>$ L $>$ 4d. At Åsa station the distance L was 70 m and d was 9 m. At Lindhov the distance L was 72 m and d was 8 m. Out of these 2 parameters the distance c is calculated using the Pythagorean theorem. The radar should stand about 1.5 meter above the rail level and horizontally aligned. The wanted height of the speed radar could not be achieved as the tripod was limited to 1.5 meter height and the rail was elevated, however as the radar still measured all the passages it should not effect the actual speeds measured and not be an issue. Looking at figure 4.4 the distances d and c was measured using a laser tool standing at the position of the radar. Pythagoras theorem and algebra then gives the distance L, in which case all

Figure 4.3: Geophone placed in a hole in the ground at Åsa station. After the unit has been leveled the hole is carefully refilled with soil and is then ready for operation.

Distance L [m]	Correction factor C for d = 5 [m]	Correction factor C for d = 10 [m]	Correction factor C for d = 20* [m]
40	1.008	1.031	1.118**
50	1.005	1.020	1.077**
60	1.004	1.014	1.054**
70	1.003	1.010	1.040**

Table 4.4: Different radar placement setups and their respective correction factors. The parameters meaning can be seen in figure 4.4.
* = not recommended distance
** = measurement errors larger than 3.5% due to radar placement

the parameters are acquired to be able to use table 4.4 and apply the correction factor on the measured speed.

The geophones and speed radar are connected to the INFRA master unit which controls the measurement tools as well as handles, saves and real time uploads the data to the Infranet server. Each sensor in the system act as a node including analog/digital signal processing, analog to digital conversion and logic. The speed radar is one sensor while the geophones consists of three sensors, one for each measured direction. After all sensors were found the master the necessary parameters, such as the standard for each geophone were set. At this stage the measurement could be started and the data would be uploaded to the project on the Infranet platform.

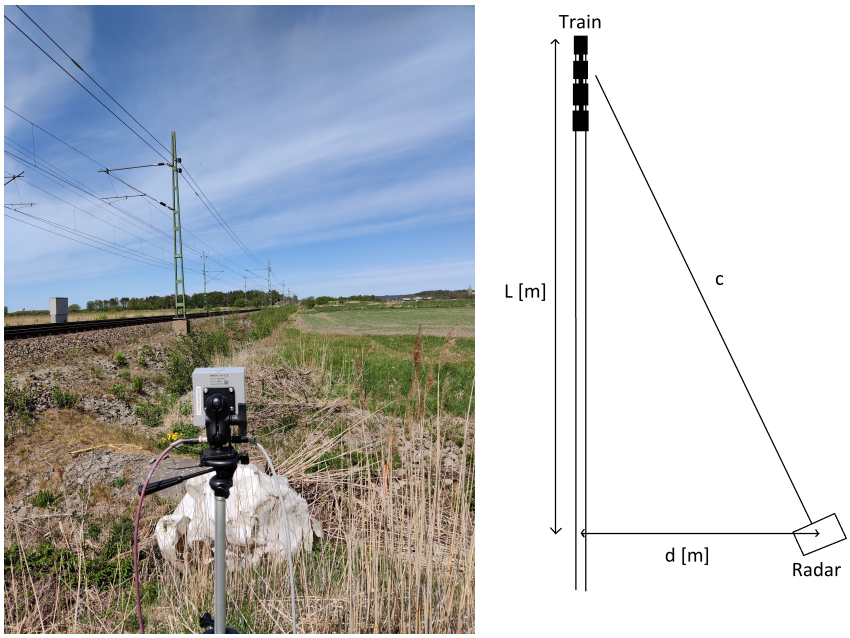

Figure 4.4: The INFRA X20SR Speed Radar at Åsa station (to the left) and a schematic picture with parameters used for calculating the correction factor (to the right).

4.3 Evaluation process

This section explains the process of evaluating the HS2 model once all measurements are done and all possible relevant data are collected. Lindhov, with a soil consisting of post glacial fine sand, had similarities to already available lithologies of the HS2 model and was as such a good candidate to evaluating the model as it is. The glacial clay at Åsa on the other hand differed greatly, enough to justify adding a new lithology to the model. The differences of the closest measurements and the source terms (also consisting of 10 m measurements) motivating these choices can be seen in figure 5.5 and 5.1 in the result section, section 5.

The goal is for the prediction of the model to be as close as possible to the measured data. The comparison tools to compare the two were:

- The root mean square error (RMSE)
- The total vibration level value of the vibrations from all frequency bands
- The maximum vibrational value difference

The root mean square error (RMSE) is a statistical measure of the differences of two outcomes, in this case predicted vibration levels of the HS2 model and the measured vibration levels. It is exactly as the name tells: take the difference between the data sets, square the error, take the mean and then the square root out of that. In the case of this thesis there is however a complication in comparing the model predictions with the measured data and that problem is the third octave bands. While both the model and the measurement devices produce output in third octave

bands the bands are not aligned. The middle frequencies of each frequency band can be seen in table 4.5.

Model freq.	-	6.3	8	10	12.5	16	20	25	31.5
Measured freq.	5.5	6.9	8.7	11	13.9	17.5	22.1	27.8	35.1
Model freq.	40	50	63	80	100	125	160	200	250
Measured freq.	44.2	55.7	70.2	88.4	111	140	177	222	281

Table 4.5: Third octave frequency bands. Highlighted in grey are the bands of the model and white are the bands of measurements.

This was solved by interpolation of the two data sets rendering them continuous. The frequency range can then be set freely, in this case of this thesis being the range of the predicted data.

The second tool of analysis is the total single value of the frequency bands, summing them up. It does not tell anything about in what range the majority of the energy lies but it is still important for the model to predict a proper single value. To compare a total single value the frequency ranges is preferably the same, at least near the same. That the frequency bands are not aligned can however cause a problem if the energy is concentrated near the boundaries of the frequency range as is the case at Åsa. 6 of the 11 valid Åsa passages on glacial clay ground can be seen in figure 4.5. The three lines represent each of the measurement points with MP1 being the closest, MP2 in the middle and MP3 furthest away. A lot of the energy there is concentrated near the lower limit of the model, around 6.3 Hz. This means that, for the calculation of the single value, it matters a lot if both the 5.5 Hz band and the 6.9 Hz band are included or only the 6.9 Hz band. Because of this two single value lines have been plotted for the Åsa measurement data, where one starts from the 5.5 Hz band and the other one starts from the 6.9 Hz band.

The last tool is the max deviation in dB between the two data sets. A small max deviation indicates for an overall reliable prediction.

Each of these tools are applicable to any arbitrary frequency range. While it is of interest to see the accuracy of the prediction as a whole, some frequency ranges are of more interest than others. With this in mind two more frequency ranges were taken into consideration. Besides the model's natural range of $6.3 - 250$ Hz, the range $6.3 - 80$ Hz as well as $6.3 - 20$ Hz were examined respectively. $6.3 - 80$ Hz is as much of the comfort range for humans as the model can cover. The main range of energy for the source terms of the model, as seen in figure 3.2 is also mainly within $20 - 60$ Hz. The same goes for the Lindhov measurements also having its vibrational energy concentrated in this range, as seen in figure 4.6. The three lines represents each of the geophones, with MP1 being the geophone closest to the rail. The most narrow and lowest range, $6.3 - 20$ Hz, gives information about the accuracy of the model relevant to vibrate buildings, as it is this range that potentially excite modes of joist in the upper floors of larger buildings. Is is also the main range of energy for the Åsa measurements, see figure 4.5. All frequency ranges were examined using

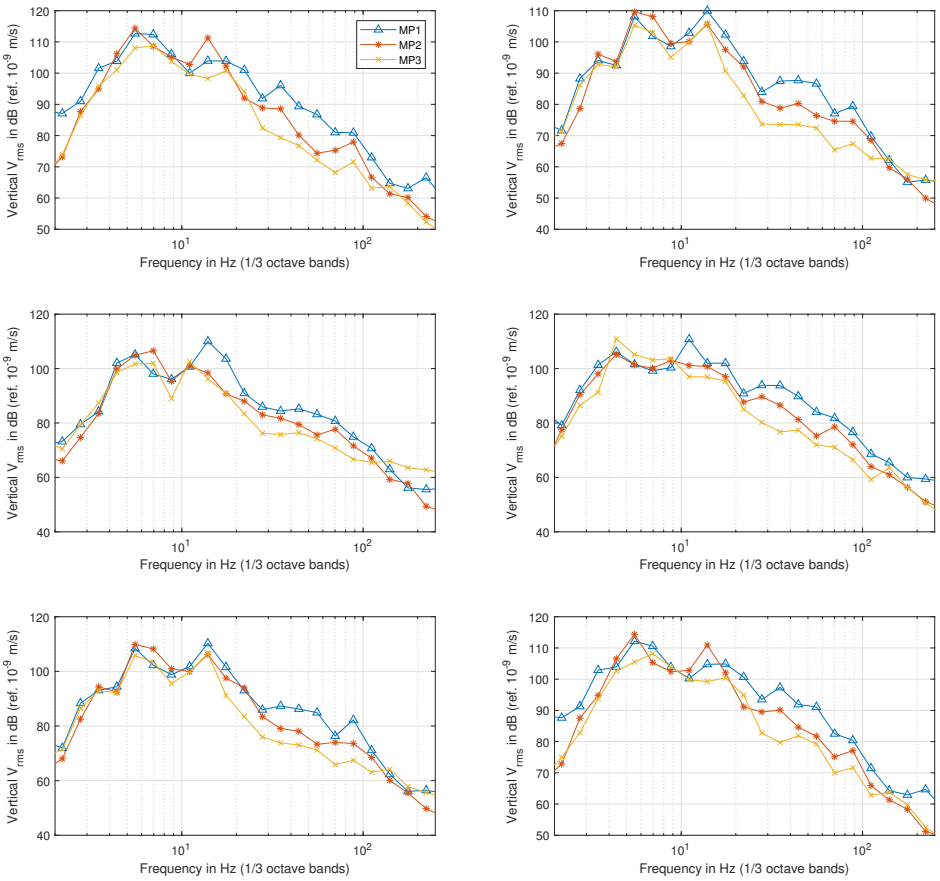

Figure 4.5: 6 arbitrary train passage at the Åsa station measurement site. Glacial clay.

the tools for each predictions made.

The majority of the predictions performed were done changing only the lithology to find out their differences and see how well they fit the measured data. For this purpose the measurement point MP3 furthest away, at 40 m or 44.5 m, was chosen. This was for multiple reasons. It is around this distance that people or buildings would be for an actual train rail. The measured data itself is also more reliable on this distance. At close distance to the excitation spot all the different wave types (see section 2.2.1) are present, which is not relevant for a building 40 m away as well as changing the measurement position just slightly can thus have a large impact on the measurement. 40 m away from the excitation the waves that propagate in all directions in the ground will have been attenuated a lot more compared to the surface traveling waves, resulting in a more reliable measurement. This fact highlights one issue of this type of measurements, being that only specific points are measured.

For each valid MP3 measurement (i.e. no missing data from measurement devices,

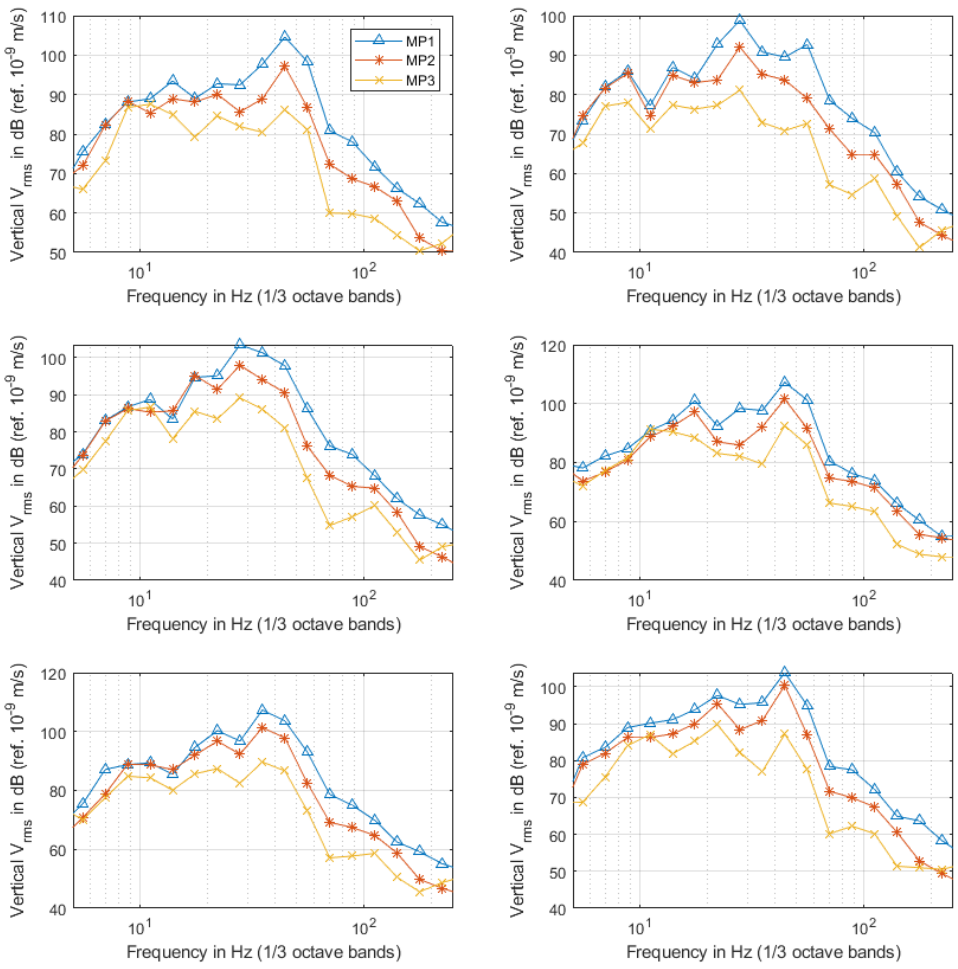

Figure 4.6: 6 arbitrary train passage at the Lindhov measurement site.

no train stopping etc) a prediction was made for each lithology. This was also done for the added "Glacial Clay" lithology for the evaluation of the Åsa station. The determined parameters speed, distance and some of the train and track dimensions were used and the undetermined parameters mass, track system and some train dimensions were set as the same for all predictions. For every one of these predictions the analysis tools were applied. The average of the passages were calculated and presented in the result section 5.

4.4 Uncertain parameters evaluation

As the correct values of a few model parameters were not acquired it is important to have in mind that the numbers from the results can only serve as quantitative indi-

cations or relative values to compare between different predictions. It could be that the prediction shows a certain lithology to be the closest to a measurement however with the correct unsprung mass it is not the case. To better deal with this an initial analysis of the weighting/impact of the unknown parameters of the model was done.

This section analyses the uncertain parameters of the model: *track system, train dimensions, weight and parabolic constants*, further explained in section 3. The results can be used to determine the uncertainty and accuracy of the predictions. It can also serve as a tool when trying to find the best prediction by modifying the uncertain parameters. The following figures shows an arbitrary prediction where all parameters are kept constant except for one of the uncertain parameters which changed.

Figure 4.7 displays changes of the train dimensions between the SJ, Regina and Öresundståg train. Because the dimensions of the trains are so similar the impact is small and essentially only applies in the lower frequencies, around 6.3 - 20 Hz. This means for the four regular lithologies of the model, see figure 3.2, the impact is very small, as the energy content there is dominant around 20-60 Hz. For a lithology where the energy content is at lower frequencies this could have a large impact, indicating the importance of further researching the train dimensions.

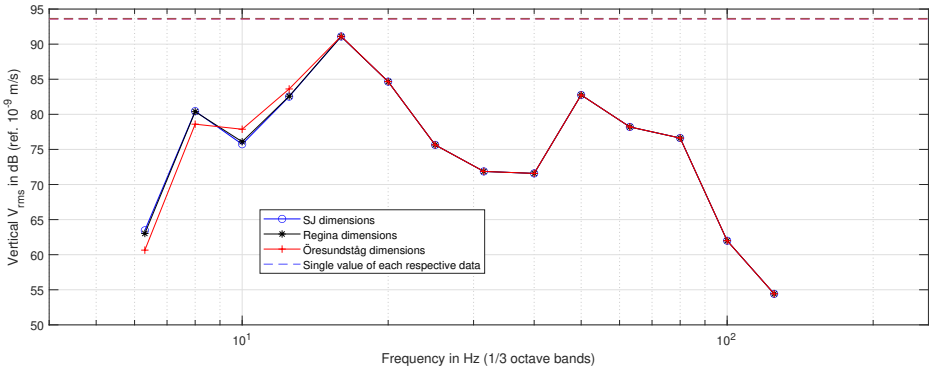

Figure 4.7: Model predictions when only changing the train dimensions.

Figure 4.8 shows the parabolic terms changing. The impact is again mainly minor but also highly frequency dependant, where it can decrease in some frequency ranges while increasing in others. As the parabolic terms is the only parameter not based on physical data from the measurement it could be changed freely to improve the prediction, however as a consequence of this it is for the best to not go too far with it. As such it was chosen to not be part of the main evaluation of the model.

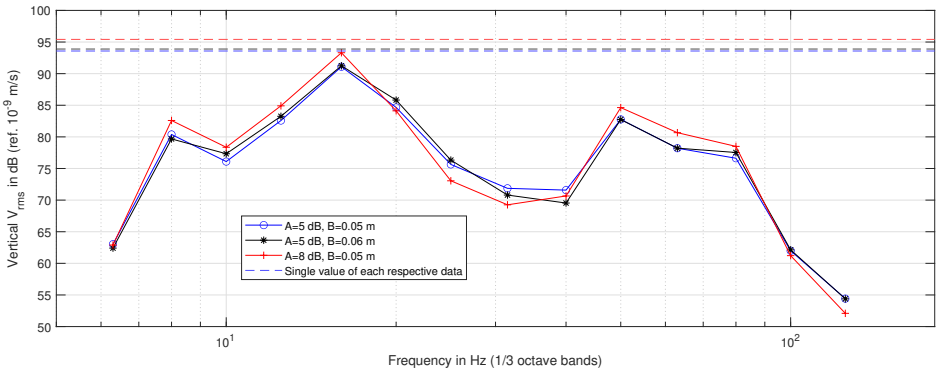

Figure 4.8: Model predictions when only changing the parabolic constants.

Figure 4.9 presents the impact of changing the track system between SNCF ballast, British ballast and the base track ballast. It is very small in the lower frequencies but gets really big with increasing frequency. Around 25 - 40 Hz the British rail prediction is almost 10 dB decreased and around 100 Hz a deviation of around 15 dB is apparent where the SNCF ballast is greatly attenuated.

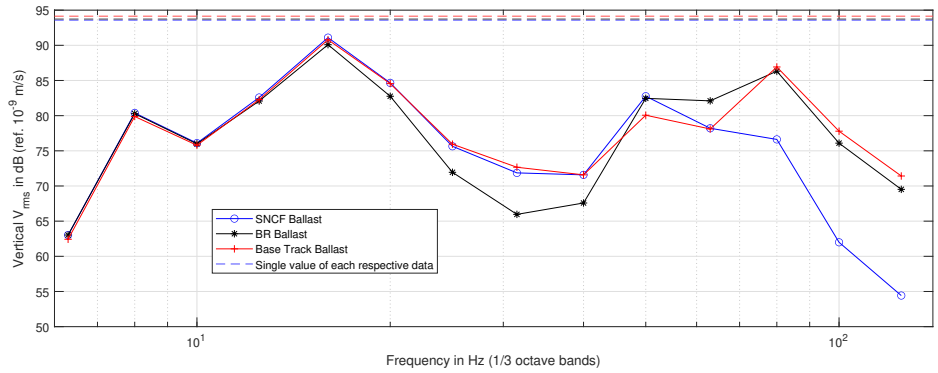

Figure 4.9: Model predictions when only changing the different track systems.

Figure 4.10 shows the predictions when changing only the unsprung mass. This is the only frequency-independent parameter impact, where a shift over the entire spectrum is the result.

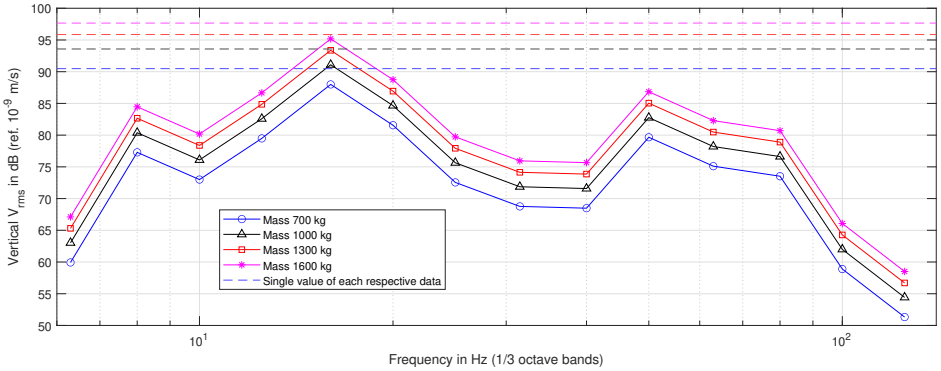

Figure 4.10: Model predictions when only changing the unsprung mass.

Something important to have in mind is the general accuracy one can expect from the model. Figure 4.11 shows 3 different passages, for each respective measurement point where the model parameters were the same for each of them, e.g. each of the 3 passages had the same lithology, speed, mass, track system and train-track dimensions. While the model will produce identical predictions for each of the passages it is clear that the actual data can differ quite a lot, around 10 dB at most in this specific example. This is due to a number of factors. One might be the service intervals where the trains and/or tracks differ in when they have been serviced to decrease the surface roughness. Another is the mass of the entire train which matters and will differentiate, not only the unsprung mass.

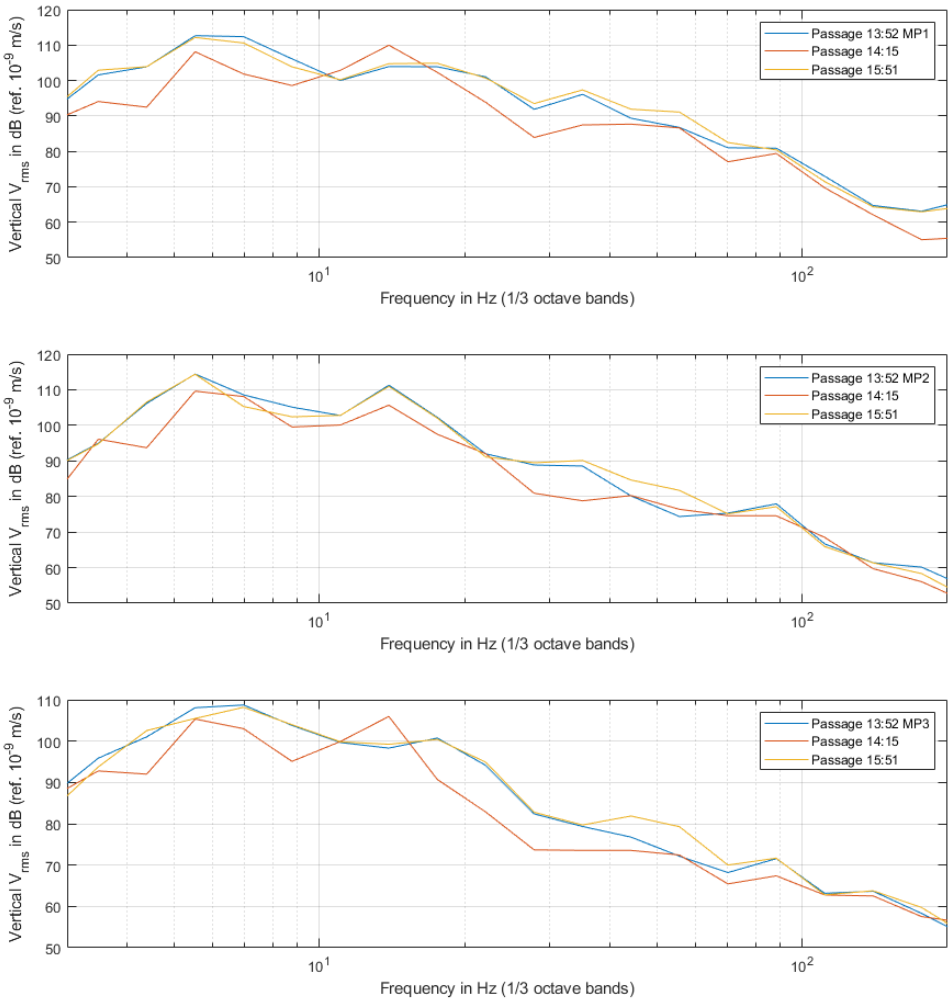

Figure 4.11: 3 passages at Åsa, for each measurement point MP1 (upper), MP2 (middle), MP3 (bottom), with equal model parameters.

4.5 Implementing additional lithology

As the glacial clay at Åsa station differed so much from the lithologies in the model a new lithology was decided to be implemented; the glacial clay lithology. This means creating new source terms as well as propagation terms.

As explained in section Model 3 the source terms are defined by the vibration levels 10 m from the railway. For this purposes the average of the measurements from MP1 at Åsa, as seen in figure 5.5, can be used. This measurements from 14.5 m distance (also MP1) was also chosen to be included. This was partly because there was small difference of the average between all MP1 and exclusively the 10 m measurements while all MP1 meant not only more underlying data in general but also a more consistent set of the data in terms of common model parameters. For the source terms themselves the only requirement is the average vibration at 10 m but the model also requires the track and train dimensions, speed and track system for the reference train used for the source terms. When including all MP1 measurements it was a heavier majority of Öresundståg and a slightly more representative average velocity (less outliers in the data set).

The propagation terms determine how the predicted vibrations differ over distance, both for geometrical attenuation and material damping. They are calculated by the function:

$$\Delta L = J(f) \cdot \log\left(\frac{R}{10}\right) + K(f) \cdot (R - 10) \tag{4.1}$$

where ΔL is the vibration difference in dB, R is the distance from the nearest rail and $J(f)$ and $K(f)$ are the lithology specific propagation coefficients, as explained in section 3. To calculate J and K the method of least squares (LSM), see section 2.4, was used. The data from all 11 valid measurements at Åsa was used, setting up ΔL as the difference between MP2 - MP1 as well as MP3 - MP1, resulting in 22 data sets for the least squares method. With the ΔL-vector and equation 4.1 the LSM matrix equation system of the shape $A \cdot b = \Delta L$ can be arranged and solved, following the method in section 2.4. The matrix equation system in this case looks like:

$$\begin{bmatrix} \log\left(\frac{R_1}{10}\right) & (R_1 - 10) \\ \log\left(\frac{R_2}{10}\right) & (R_2 - 10) \\ \vdots & \vdots \\ \log\left(\frac{R_{22}}{10}\right) & (R_{22} - 10) \end{bmatrix} \cdot \begin{bmatrix} J \\ K \end{bmatrix} = \begin{bmatrix} \Delta L_1 \\ \Delta L_2 \\ \vdots \\ \Delta L_{22} \end{bmatrix} \tag{4.2}$$

where R_1 to R_{11} is 20 m and R_{12} to R_{22} is 40 m. The calculated values for the source terms and propagation terms can be seen in the result section, see 5.2.

5
Results and Discussion

This section is divided into 5 different parts. The first part will show the results of the *Lindhov* evaluation and how the model can predict the passages of that ground type. Following is a section presenting the *glacial clay* lithology addition. This will then be applied to the *Åsa* predictions too see how it performs. Lastly is a section about ideas for continued works.

5.1 Lindhov

Figure 4.6 in the method section shows 6 of the 8 regular Lindhov passages, arbitrarily chosen, where the lithology is post glacial fine sand. The three lines represents each of the geophones, with MP1 being the geophone closest to the rail. The magnitude of the vibrations decrease with increased distance. The area of most energy and the peaks are approximately around 28-45 Hz on all of the measurements. The magnitude at MP1 is generally around 100-110 dB where the difference of magnitude between passages mainly depends on the speed differences of the passing trains. An interesting observation is that at lower frequencies, below around 15 Hz, the magnitude does not always decrease with distance. This is likely due to resonances in the soil layer between the with the bedrock and the free ground surface. The soil layer at Lindhov is 5-10 m. The depth as well as typical sand wave speeds, see table 2.3, can be used to find ground resonances, see equation 2.9. The first mode eigenfrequencies, assuming medium-firm sand with 5 - 10 m ground layer depth, are found at frequencies between 5 to 15 Hz.

Lindhov had 3 freight train passages as well as a passage with a single locomotive. These passages were of low interest as they did not cause any large vibration levels compared to the passage trains. They were as such not further evaluated. Freight train are however usually of interest because of their mass as well as their length and speed usually resulting in a long lasting passage, one that can be more disturbing for people compared to a passage train. In this case the speed and mass were too low to create any vibrations of interest. The levels can be seen in the transient report in Appendix A.

The spectra at the first geophone, MP1, at 10 or 14.5 m from the near or distant track, from the Lindhov measurements can be seen in figure 5.1. The energy content is in this case much more coherent with the source data of the HS2 model, with a peak around 40 Hz. The thick red line is the average of the blue MP1 passages

and has similar shape to that of the 'Sand Clay' as well as the 'Sand' curve. The Lindhov soil itself consists of "postglacial finsand". Generally the character of the measured data (blue lines) are quite consistent and the model seems to be compatible with the ground type.

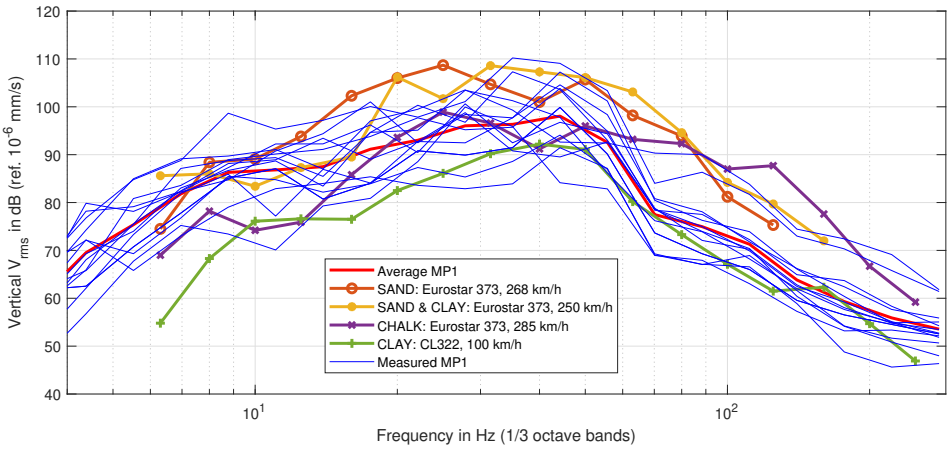

Figure 5.1: MP1 measurements at Lindhov (blue lines), their average (red line) as well as the reference source spectra for the model.

An example of a few model predictions compared to the measured data can be seen in figure 5.2. It shows the first passage at Lindhov and how each lithology of the model predicted the vibrations. Here the 'Sand' lithology was the most accurate with an RMSE value of 7.4 dB, single value difference of 0.7 dB and a max deviation of 13.3 dB.

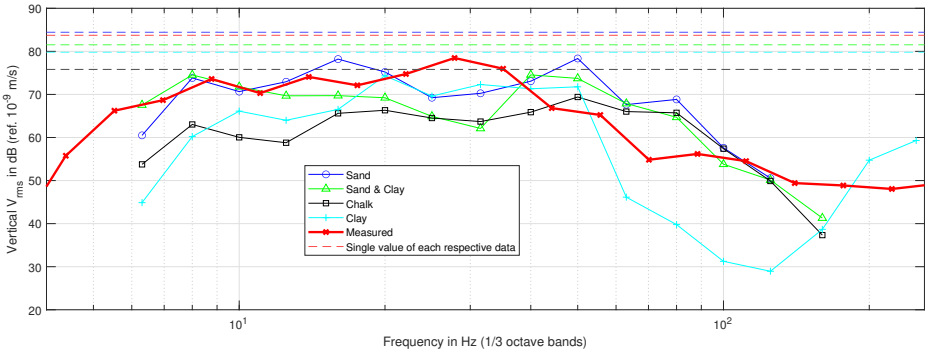

Figure 5.2: Passage 14:50 at Lindhov. Showing the measured data from MP3 as well as predicted values from the model. The dashed lines are the equivalent values for the entire frequency range for each data set.

Table 5.1 presents the average values of all 8 regular Lindhov passages of the evaluation tools presented in the method section 4.3. In general the lithologies 'Sand Clay' and 'Sand' performed the best. The RMSE values were similar for them both, with 'Sand Clay' slightly outperforming 'Sand' with around 0.6-2 dB better results

per evaluated frequency range. The prediction is better when the whole frequency range is taken into consideration, and about the same when its only up to 20 Hz. In terms of single value 'Sand' predicted very well, while 'Sand Clay' was around 5 dB off. The single value being negative indicates the model prediction being lower than measurement value. For the max deviation 'Sand Clay' predicted best, with 'Sand' having similar results. The max deviation appears somewhere in the 20-80 Hz region. It is again important to have in mind that since not all parameters are known the actual values are bound to alter with more accurate parameters and that the focus is to compare the lithologies against each other.

	Sand	**Sand & Clay**	**Chalk**	**Clay**
RMSE	8,60	7,68	9,56	13,79
RMSE 80	9,68	10,20	12,62	10,67
RMSE 20	5,42	4,98	13,34	11,65
Single value	-1,63	-5,68	-11,09	-7,63
Single value 80	-1,61	-5,67	-11,12	-7,64
Single value 20	-0,48	-4,99	-12,12	-7,35
Max diff	16,85	17,81	21,89	26,62
Max diff 80	16,85	17,81	21,89	25,51
Max diff 20	11,59	8,69	20,15	25,51

Table 5.1: The results of the evaluation tools in dB, presented in section 4.3, applied to each of the 8 Lindhov passages and then averaged. RMSE is the root mean squared error between the measured vibration level and the predicted, single value is the broadband vibration level and max diff is the maximum deviation between the measured and predicted vibration level. When the single value is negative means the model prediction is lower than the measurement value.

5.2 Glacial clay lithology

Table 5.2 shows the calculated source terms used in the HS2 model for the implemented glacial clay lithology. The source terms can also be seen together with the other source terms of the other ground types in figure 5.3. The dominant energy content is concentrated in the lower frequencies, around 6.3 - 16 Hz, corresponding to the character of the measured data at Åsa, as can be seen below in figure 4.5. The source terms are based on all regular MP1 passages at Åsa, meaning all train types are included. There were mainly Öresundståg passing but also a few SJ trains, however none of the stopping trains. Arguably it would be better to create a new lithology with a corresponding train type using only source data from one train type, nonetheless this was decided on as the train dimensions are all very similar according to the data available. This is still however to be considered an uncertainty. The speed of the new lithology is also chosen as the average speed of all the passages. Another important thing to have in mind is that all the reference train attributes are different than the reference of the other model lithology choices. This means that the reference weight in the unsprung mass correction factor is not anymore 1000 kg as it is in the model, but the unsprung mass of the Öresundståg/SJ train. With

all this said, even with more certainty in the underlying data the source terms and propagation term should be based from more measurement sites. Partly because generally more data is required to acquire a reliable model but also because a single glacial clay site does not represent all of them.

Freq.	6.3	8	10	12	15	20	25	31.5	40
Prop. terms	103.07	100.30	101.02	104.42	104.12	97.36	90.95	89.09	88.40
Freq.	50	63	80	100	125	160	200	250	
Prop. terms	86.35	82.66	78.37	73.54	67.04	60.65	58.69	58.22	

Table 5.2: Source terms for post glacial clay.

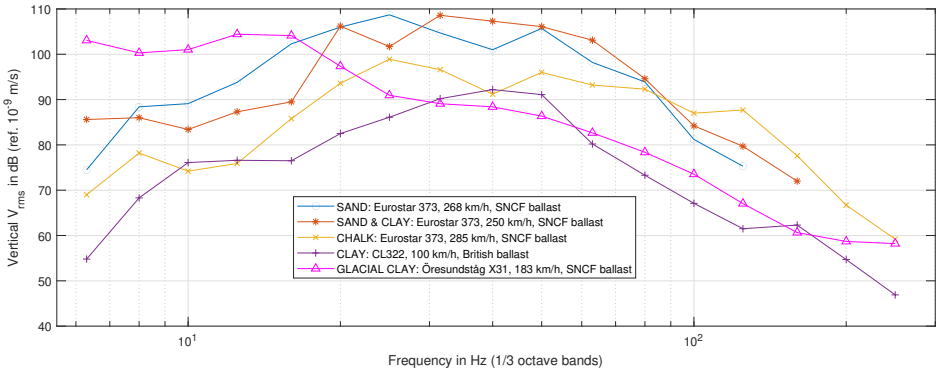

Figure 5.3: The HS2 reference source terms with the added glacial clay lithology.

Table 5.3 show the propagation terms for the glacial clay implementation. Figure 5.4 shows the propagation factor ΔL and how it changes over distance (upper in the figure), for each of the 17 third octave bands. For comparison the propagation for the Sand Clay lithology is presented (middle) as well as data from an analysis report for Ostlänken (lower) [22]. The report investigates and calculates new glacial clay source terms for the HS2 model as well. As can be seen for glacial clay some bands are increasing over distance, few of them drastically increasing, which is not an expectable effect in real life. The four lines that are the most increasing at 80 m corresponds to the four frequency bands 125 Hz, 160 Hz, 200 Hz and 250 Hz. This will unlikely be the actual coefficients for an established final version of the propagation factors, however as can be seen in figure 4.5 it is the case that amplitude can increase over distance in this specific case. This is further discussed in the following section. Another observation is that the energy attenuation is less then that of the Sand Clay which also is the lithology with the least attenuation of the HS2 lithologies. This is reinforced by comparing the Åsa passages data, figure 4.5 and the Lindhov passages data, figure 4.6, where the geometric attenuation and material damping is more evident for the Lindhov passages.

Freq.	6.3	8	10	12	15	20	25	31.5	40
J	20.42	7.96	-3.65	-13.92	-37.18	-16.91	1.11	-20	-40.28
K	-0.33	-0.27	-0.01	-0.02	0.43	0.08	-0.38	-0.02	0.43
Freq.	50	63	80	100	125	160	200	250	
J	-56.09	-14.43	-17.19	-27.69	-43.24	-23.71	-83.80	-82.10	
K	0.74	-0.07	0.02	0.33	0.72	0.55	1.65	1.59	

Table 5.3: Propagation coefficients for post glacial clay.

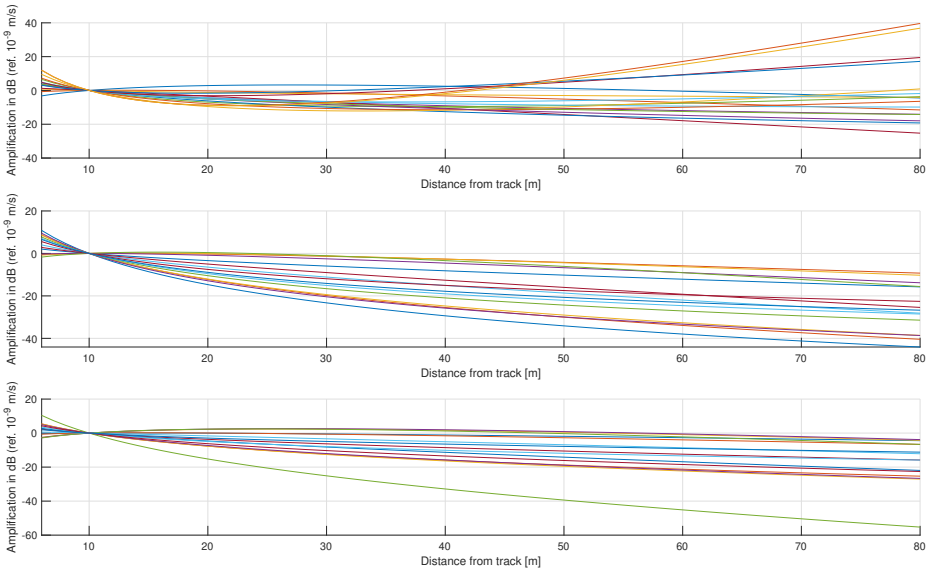

Figure 5.4: Propagation terms for the added glacial clay lithology (top), the sand clay lithology in the HS2 model (middle) and for the glacial clay of the Ostlänken project [22].

5.3 Åsa

6 of the 11 valid Åsa passages on glacial clay ground can be seen in the method section, in figure 4.5. The majority of the energy content is around 4 - 20 Hz, meaning its centered at the lower limit of the model and to some degree outside its range. This is problematic and indicates towards extending the range of the model for compatibility of the Swedish glacial clay. Another interesting observation is the attenuation over distance, or rather the lack it. Around 20 Hz is when the lack of attenuation is noticeable and at lower frequencies two out of the three lines often coincides. It is also not always MP1 that has the highest levels. One relevant factor here is the setup of the measurement points, which unlike Lindhov is not setup in a straight line but more separated, see figure 4.1. This means the waves propagate through slightly different path with, to some extent, different properties. The ground was generally quite rock filled when digging the holes for the geophones which also means irregularities compared to a compound homogeneous soil. One

other possible explanation to the behaviour, similar to Lindhov, is resonances in the ground between the surface and bedrock as explained in theory section 2.2.6. This is however less likely as the shear wave speed is decreased for the loose soil as well as the depth. The first eigenfrequencies are more likely around 3 Hz.

The Åsa measurements consisted of 5 passages of trains stopping at the nearby Åsa station. These passages were not further evaluated as they did not result in any relevant vibration levels. The measurement spots were placed connecting to the acceleration interval of the trains, which is of interest as acceleration can also give rise to large vibrations. This was however not the case during the Åsa measurements.

Figure 5.5 shows the spectra from the measurements done at Åsa station as well as their average, at the first geophone MP1, i.e. at a distance of 10 or 14.5 m from each respective track. There are 11 passages in total and the general character of the measured data is rather consistent between the passages. There are usually two peaks, more or less apparent, around 5 and 14 Hz approximately. The differences in magnitude likely mostly depend on the speed of the trains and the distance. The magnitude varies in range of up to 20 dB (around 5 Hz) and the speed range is 148 - 198 km/h. The energy content is heavily shifted between the spectra of the HS2 source data and the measured data where the measured data has its peaks near or below the lower limit of the source data (being the lower limit of the HS2 model). While the distance differences of 10 and 14.5 m are relevant it does not justify separating the data and wouldn't change the results significantly.

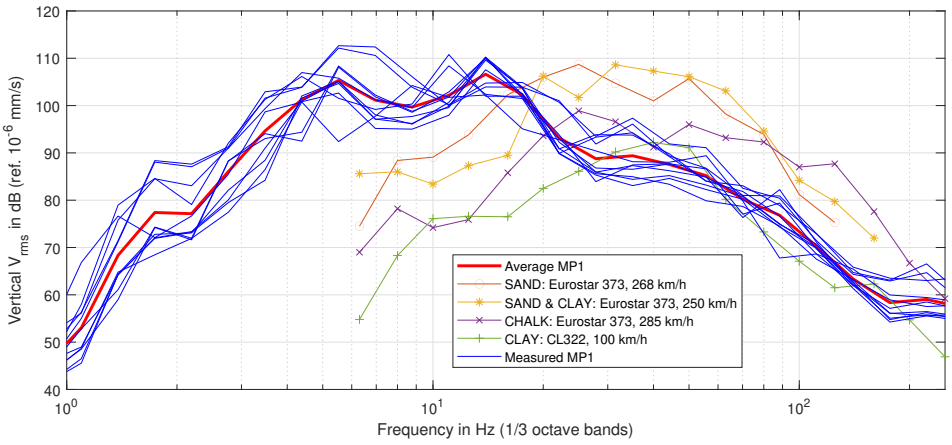

Figure 5.5: MP1 measurements at Åsa (blue lines), their average (red line) as well as the reference source spectra for the model.

An example of model predictions compared to the measured data can be seen in figure 5.6. It shows the fourth passage at Åsa and how each lithology of the model predicted the vibrations. Here the 'Glacial Clay' lithology was the most accurate with an RMSE value of 2.7 dB, single value difference of 0.6 dB and a max deviation of 9 dB.

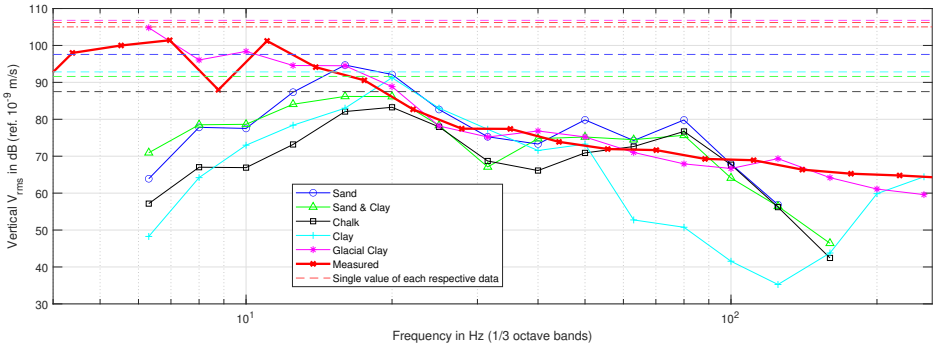

Figure 5.6: Passage 14:27 at Åsa, showing the measured data from MP3 as well as predicted values from the model. The dashed lines are the single value for the entire frequency range for the modeled data and starting on either 5.5 Hz (red dashed line) or 7 Hz (red dash-dotted line).

Table 5.4 presents the average of all 11 regular Åsa measurements evaluated with the tools of section 4.3. This time the addition of the Glacial Clay lithology has been added. It highly outperforms all of the other lithologies. Although that is expected as it is been derived directly from the measurements its being tested against, it is still confirmation of the legitimacy of the new lithology being done correct. Both the average RMSE and single value predicts within a few dB for each respective frequency range. The single value predicting even better when skipping the first point of the measurement data to calculate the single value (not shown in the table). The max deviation stays below 10 dB as well, which means a reliable accuracy over the entire frequency range. Comparing this with figure 4.1, the same passage, from the perspective of the model, can still have a 10 dB difference as seen. Besides 'Glacial Clay' the predictions exhibits rather similar to the Lindhov predictions. 'Sand' and 'Sand Clay' performed second best and rather similar while 'Chalk' and 'Clay', in this case, drastically fall behind.

	Sand	Sand & Clay	Chalk	Clay	Glacial Clay
RMSE	7,74	8,34	10,98	16,19	3,47
RMSE 80	8,50	8,14	11,95	13,96	2,63
RMSE 20	15,52	15,60	24,63	23,63	3,68
Single value	-11,25	-16,77	-21,17	-15,90	-1,61
Single value 80	-11,25	-16,78	-21,22	-15,90	-1,61
Single value 20	-11,69	-17,53	-22,86	-16,81	-1,61
Max diff	39,07	31,73	45,71	54,55	8,33
Max diff 80	39,07	31,73	45,71	54,55	8,28
Max diff 20	39,07	31,73	45,71	54,55	8,02

Table 5.4: The results of the evaluation tools in dB, presented in section 4.3, applied to each of the 11 Åsa passages and then averaged. RMSE is the root mean squared error between the measured vibration level and the predicted, single value is the broadband vibration level and max diff is the maximum deviation between the measured and predicted vibration level. When the single value is negative means the model prediction is lower than the measurement value.

5.4 Greby

This section shows how the model and the implemented glacial clay source spectrum performs for measurements made at Greby, Skövde. The data comes from 2009, supplied by Efterklang - part of AFRY and is the same data as the one used in Gustav Vågfelt's thesis. It is mainly to see the performance of the glacial clay lithology, but is including all of the lithologies for comparison. The data used were 3 passages measured at a distance of 10 m and 25 m. All of them used one train type being the Regina train at a speed of 150, 200 and 250 km/h. This means a total of 6 measurements were used when evaluating the model for Greby. Figure 5.7 shows the passage at a 10 m (top) and a 25 m (bottom) distance.

Figure 5.8 shows the spectra from the measurements at Greby and some of the measurements from Åsa. As can be seen, and has already been pointed out, the increasing distance at Åsa does not necessarily result in decreased vibration levels. The Greby measurements however have a significant level decrease over distance. The soil layer at Greby is 3 - 5 m according to Geomap. This is the depth where resonances are expected to give rise to magnitude amplifications for the glacial clay ground type. That is however not what is seen in the results. This indicates further geological reasons are behind the behaviour, meaning that further geological research is needed. There is also no data of the meteorological conditions during the Greby measurement, only that it was done in June.

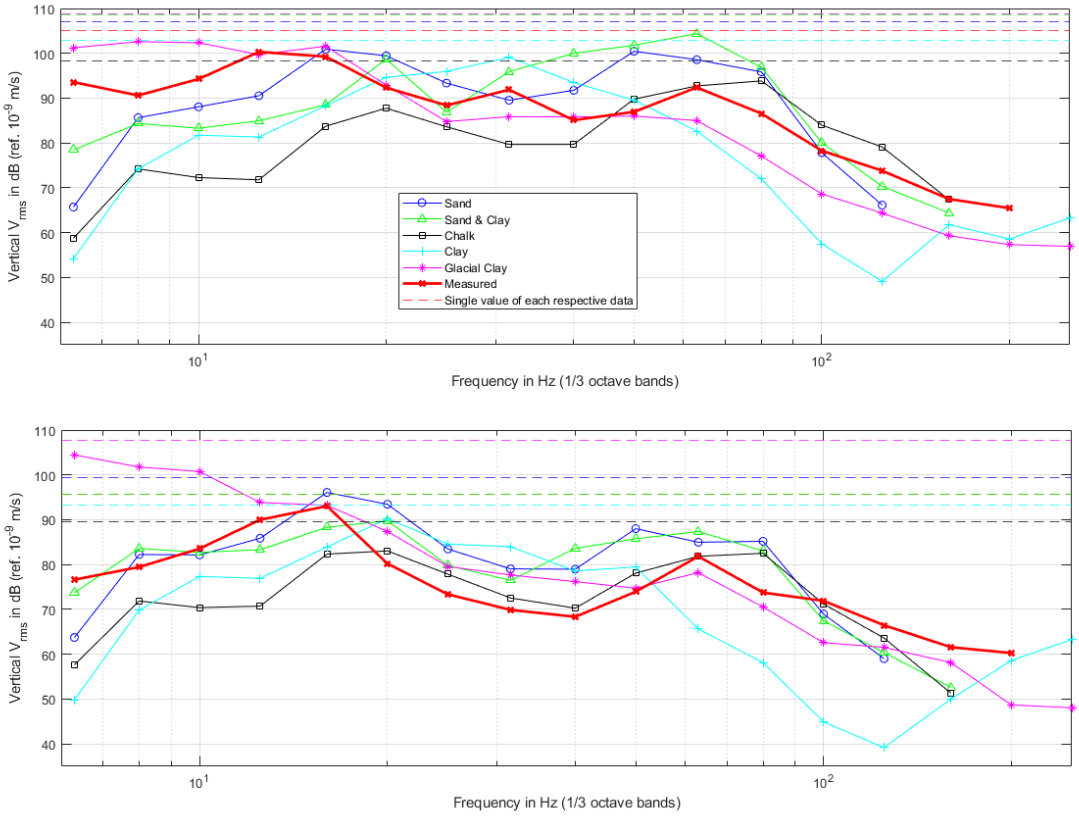

Figure 5.7: Passage at Greby, showing the measured data as well as model predictions for each lithology at a distance of 10 m (top) and 25 m (bottom). The dashed lines are the single value for the entire frequency range for each respective data.

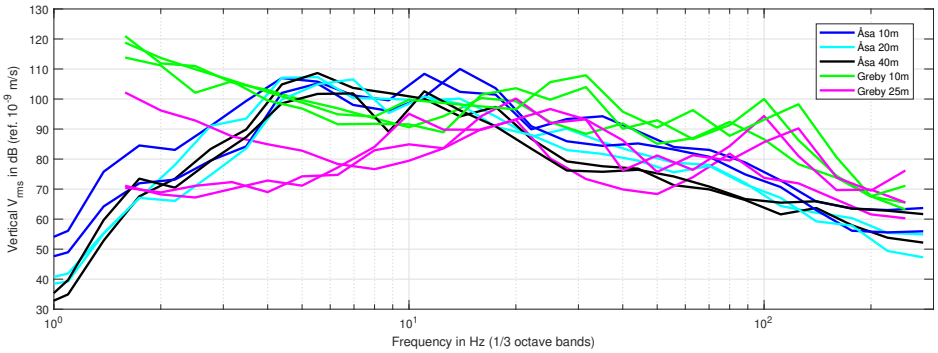

Figure 5.8: Measurements from Greby at 10m and 25m, as well as measurements from Åsa at 10m, 20m and 40m.

	Sand	Sand & Clay	Chalk	Clay	Glacial Clay
RMSE	7.19	7.91	7.35	17.26	9.49
RMSE 80	7.33	8.98	8.23	12.57	7.73
RMSE 20	6.88	6.98	16.39	13.30	9.16
Single value	1.72	0.23	-8.09	-1.41	6.10
Single value 80	1.82	0.32	-8.25	-1.31	6.20
Single value 20	1.38	-3.04	-11.75	-5.73	7.61
Max diff	19.80	16.13	26.19	35.21	22.85
Max diff 80	19.58	15.24	26.19	33.23	21.86
Max diff 20	19.45	12.17	26.19	32.08	19.80

Table 5.5: The results of the evaluation tools in dB, presented in section 4.3, applied to each of the 6 Greby passages and then averaged. RMSE is the root mean squared error between the measured vibration level and the predicted, single value is the broadband vibration level and max diff is the maximum deviation between the measured and predicted vibration level. When the single value is negative means the model prediction is lower than the measurement value.

5.5 Continued work

There are a lot of ways this thesis can be continued, ranging from essentials ones to ones for quality of life purposes. The most important is to continue gathering data from different Swedish train passage measurement sites with different lithologies and apply the evaluation tools on it. Further evaluation is needed, both to confirm the models applicability on the already available lithologies, as well as to evolve and confirm the added glacial clay lithology. The model should be tested against well analysed lithologies to get a better picture of its accuracy as well as an understanding of how it should be calibrated. This is extra important when continuing the work of the glacial clay source terms as it could play an important role in explaining the behaviour of the propagation attenuation of the glacial clay. The reliability of it is not sufficient and to make it more reliable the geological aspect of the evaluation is important. An important thing to have in mind though, is that the model is empirical and meant to be used as an early stage measure to get an estimation of the vibration levels. This typically means a thorough lithology investigation is not available, implying minor knowledge of the lithology should be required to apply the model. It is therefor important that the model predicts accurate without too much fine tuning of the parameters, e.g. the parabolic constants.

A fair amount of data needed in the model is still missing and/or uncertain where further research is needed. The unsprung mass is one of the largest and most important unknowns, also being the hardest to find data on. Unfortunately multiple Swedish train related organisations, such as Trafikverket, Transportstyrelsen and the respective train operating companies did not have the information. A great possible asset to have would be a database with all the HS2 model related train data.

As glacial clay has dominant energy in the lower frequency range, even below the lower limit of the model, an extension of the frequency range at the lower limit would be a great addition to the model in order to make it more applicable to loose clay.

There is also the possibility for improvements on making the model more user friendly by implementing a GUI (graphical unit interface). This would not require a lot of sophistication as the model is rather straight forward and linear. It could consist of a single window page with each parameter of each step of the model as input producing a final graph and vector in the end. It could perhaps take reference data as input for comparison as well, possibly including evaluation tools.

The scope of the implementation of the model could also be expanded on to cover more steps of the model. The branches in figure 3.1 of the section types could be included, i.e. "Bored tunnel" and "Cut Cover tunnel". Building response could also be implemented as well as evaluated under Swedish conditions.

The model is using a generic roughness profile, the same one for each lithology as roughness level for the reference data were not available. It indicates that the used roughness profile should be fairly applicable in Sweden, however it could be worth to compare it to Swedish tracks. Best would be to make a roughness measurement of the track of interest.

6
Conclusion

This study aimed to evaluate the performance of the HS2 model in predicting vibration levels in Swedish lithologies, with a focus on post glacial fine sand and glacial clay. Overall, the thesis successfully followed the aim, and the results revealed some interesting findings.

The measurements taken at Åsa showed different characterization of vibration levels, especially in the lower frequencies where the energy was concentrated. Comparing the measurement data between the Åsa and Greby measurement, both having the glacial clay soil, deviations in the distance dependency occurred which requires further analysis to determine the cause.

For fine sand, the HS2 model's predictions were quite accurate and reliable with consistent deviations, which could be managed. However, for glacial clay, it was clear from the early stages of the study that the HS2 model needed to be expanded to better define the source and propagation terms. The propagation terms of the implemented glacial clay lithology showed significant differences in behavior compared to other source terms of model, further indicating that it requires more underlying data to make it an established addition to the model.

The study also highlighted the need for more data to properly evaluate the HS2 model's performance. Specifically, additional measurements are required to test the model's accuracy against different lithologies. Furthermore, sources of error in the data, such as missing data and frequency misalignment, need to be addressed.

In conclusion, this study provides new data, source terms and evaluation tools for the HS2 model and highlights the need for further research to refine the accuracy and applicability of the HS2 model.

Bibliography

[1] G. Vågfelt "Empirical prediction of ground-borne vibration from railway systems", 2021 [Online] Available: https://odr.chalmers.se/items/f9b48d43-20cf-42bc-8bb5-52255a9456e6

[2] Puggen, *"File: SJ2000 Gamla Uppsala.jpg" Wikimedia Commons* [Online], September 2010. Available: https://commons.wikimedia.org/wiki/File:SJ2000_Gamla_Uppsala.jpg

[3] Linear regression, *"Normdist_regression.png" Wikimedia Commons*[Online], October 2007. Available: https://commons.wikimedia.org/wiki/File:Normdist_regression.png

[4] "London - West Midlands Environmental Statement" - High Speed Two Limited, England, Volume 5 Appendix SV-001-000 ES 3.5.0.10, Nov 2013. [Online] Available: ://webarchive.nationalarchives.gov.uk/ukgwa/20140613014254/http://assets.dft.gov.uk/hs2-environmental-statement/volume-5/sound/Vol5$_{A}ppendix_{S}V-001-000.pdf$

[5] "London - West Midlands Environmental Statement" - High Speed 2 Limited, England, Volume 5 Appendix SV-001-000 ES 3.5.0.15, July 2017. [Online] Available: http://assets.dft.gov.uk/hs2-environmental-statement/volume-5/sound/Vol5_Appendix_SV-001-000.pdf

[6] "High Speed Rail (West Midlands - Crewe) Environmental Statement," High Speed Two Limited, England, Volume 5 Appendix SV-001-000 ES 3.5.0.15, Jul. 2017. [Online] Available: https://assets.publishing.service.gov.uk/government/uploads/system/uploads/attachment_data/file/628750/E61_SV-001-000_WEB.pdf

[7] "Crossrail Information Paper, D10 - Groundborne Noise and Vibration", Crossrail, Londong, England, Apr. 2008. [Online] Available: https://2577f60fe192df40d16a-ab656259048fb93837ecc0ecbcf0c557.ssl.cf3.rackcdn.com/assets/library/document/d/original/d10groundbornenoiseandvibration.pdf

[8] "Buildings: Vibration and shock, evaluation of annoyance (NT ACOU 082)" May 1991. [Online] Available: http://www.nordtest.info/wp/1991/05/15/

buildings-vibration-and-shock-evaluation-of-annoyance-nt-acou-082/

[9] N. Triepaischajonsak, D. Thompson, C.J.C. Jones, J. Ryue and J.A. Priest, "Ground Vibration from Trains: Experimental Parameter Characterization and Validation of a Numerical Model," Proceedings of the Institution of Mechanical Engineers Part F Journal of Rail and Rapid Transit 225(2):140-153, Mar. 2011. [Online] Available: https://www.researchgate.net/publication/258177602_Ground_Vibration_from_Trains_Experimental_Parameter_Characterization_and_Validation_of_a_Numerical_Model

[10] "High Speed 2" *High speed 2 Ltd 2021*, 2021 [Online] Available: https://www.hs2.org.uk/

[11] "Geomap" *Geological Survey of Sweden.* [Online] Available: https://apps.sgu.se/geokartan/#mappage

[12] "Website: https://www.sigicom.se/produkter/vibration-sv/infra-v12-triaxiell-geofon/

[13] "Website: https://www.sigicom.com/products/geotech/infra-x20sr-speed-radar/

[14] "SGF Informationsskrift 1:2012 Markvibrationer Version 2013-12-18" (text in Swedish), *Swedish Geotechnical Society*, Dec. 2013. [Online] Available: http://www.sgf.net/getfile.ashx?cid=495387&cc=3&refid=5

[15] Website: Efterklang™, part of AFRY webpage https://afry.com/en/area/acoustics-sound-design

[16] Website: Trafikverket https://www.trafikverket.se/

[17] Website: Transportstyrelsen https://www.transportstyrelsen.se/sv/vagtrafik/

[18] Website: University of Gothenburg https://gmv.gu.se/urbanfutures/sv/projekt/urbana-stationssamhallen

[19] *Mechanical vibration - Ground-borne noise and vibration arising from rail*, ISO 14837-1:2005

[20] *"Earthquakes: 'Newly Revised and Expanded'"* Bolt, B.A. W.H. Freeman Company, New York, 1993.

[21] V.V. Krylov (editor), *Noise and Vibration from High-Speed Trains,* London, England: Thomas Telford Limited, 2001.

[22] Anders Lindgren, *PM Vibrationer från höghastighetståg, Analysrapport utifrån utförd vibrationsmätning jan 2020,* Filnamn: OLP0-04-025-00000-0_0-1018 Trafikverket

[23] Website: Trafikverket `https://www.trafikverket.se/resa-och-trafik/jarnvag/Sveriges-jarnvagsnat/`

[24] "Glaciala finkorniga sediment" (text in Swedish), *Geological Survey of Sweden.* [Online] Available: `https://www.sgu.se/om-geologi/jord/fran-istid-till-nutid/isen-smalter/glaciala-finkorniga-sediment/`

[25] "Railway Induced Vibration" *International union of railways*, Nov 2017 [Online] Available: `https://uic.org/IMG/pdf/uic-railway-induced-vibration-report-2017.pdf`

[26] *Vibrations and shock - Evaluation of human exposure to whole-body vibration*, ISO 2631.

A

Appendix 1

Transientrapport

Projekt	Markvib tåg Jim exjobb Åsa Station
Projektansvarig	Gustav Vågfelt
Tidsspann	2022-05-16 13:40 - 2022-05-16 17:00 (Europe/Stockholm)

Mätpunkt	MP_1	MP_2	MP_3
Plats	-	-	-
Sensortyp	V12	V12	V12
S/N	3510	2980	20810
Logger S/N	1746	1746	1746
Senaste kalibrering	2021-04-23	2021-04-23	2020-10-13
Standard	Geophone 5000µm/s 5-500Hz	Geophone 5000µm/s 5-500Hz	Geophone 5000µm/s 5-500Hz
Enhet	um/s	um/s	um/s
Storhet	Velocity	Velocity	Velocity
Intervalltid	2 min	2 min	1 min

Datum/Tid	MP_1 - V12	MP_2 - V12	MP_3 - V12
2022-05-16 16:55:53	2022-05-16 16:55:53 V: 223 um/s, 17.1 Hz L: 126 um/s, 7.43 Hz T: 109 um/s, 6.77 Hz	2022-05-16 16:55:53 V: 194 um/s, 9.51 Hz L: 166 um/s, 8.62 Hz T: 149 um/s, 6.83 Hz	2022-05-16 16:55:53 V: 126 um/s, 6.68 Hz L: 76 um/s, 14.8 Hz T: 84 um/s, 6.30 Hz
2022-05-16 16:50:48	2022-05-16 16:50:48 V: 1110 um/s, 12.4 Hz L: 635 um/s, 13.7 Hz T: 377 um/s, 11.5 Hz	2022-05-16 16:50:48 V: 897 um/s, 8.37 Hz L: 677 um/s, 14.5 Hz T: 977 um/s, 11.5 Hz	2022-05-16 16:50:48 V: 595 um/s, 8.39 Hz L: 419 um/s, 13.2 Hz T: 450 um/s, 7.47 Hz
2022-05-16 16:38:59	2022-05-16 16:38:59 V: 275 um/s, 12.8 Hz L: 121 um/s, 6.49 Hz T: 119 um/s, 6.33 Hz	2022-05-16 16:38:59 V: 208 um/s, 8.80 Hz L: 157 um/s, 7.20 Hz T: 143 um/s, 6.02 Hz	2022-05-16 16:38:59 V: 128 um/s, 5.60 Hz L: 71 um/s, 7.72 Hz T: 62 um/s, 6.70 Hz
2022-05-16 16:35:03	2022-05-16 16:35:03 V: 1240 um/s, 11.1 Hz L: 656 um/s, 11.1 Hz T: 612 um/s, 9.27 Hz	2022-05-16 16:35:03 V: 1030 um/s, 8.66 Hz L: 794 um/s, 13.3 Hz T: 1270 um/s, 12.0 Hz	2022-05-16 16:35:03 V: 887 um/s, 10.7 Hz L: 560 um/s, 11.0 Hz T: 761 um/s, 9.47 Hz
2022-05-16 16:29:43	2022-05-16 16:29:43 V: 157 um/s, 9.02 Hz L: 35 um/s, 9.71 Hz T: 23 um/s, 9.13 Hz	2022-05-16 16:29:43 V: 29 um/s, 9.01 Hz L: 14 um/s, 9.75 Hz T: 10 um/s, 9.06 Hz	2022-05-16 16:29:43 V: 9 um/s, 7.66 Hz L: 3 um/s, 9.23 Hz T: 4 um/s, 183 Hz
2022-05-16 16:23:37	2022-05-16 16:23:37 V: 218 um/s, 8.82 Hz L: 171 um/s, 10.4 Hz T: 147 um/s, 8.27 Hz	2022-05-16 16:23:37 V: 279 um/s, 7.38 Hz L: 196 um/s, 7.25 Hz T: 178 um/s, 7.47 Hz	2022-05-16 16:23:37 V: 105 um/s, 6.88 Hz L: 81 um/s, 6.89 Hz T: 76 um/s, 7.92 Hz
2022-05-16 16:08:13	2022-05-16 16:08:13 V: 1210 um/s, 10.7 Hz L: 807 um/s, 7.29 Hz T: 659 um/s, 6.79 Hz	2022-05-16 16:08:13 V: 852 um/s, 7.33 Hz L: 843 um/s, 6.34 Hz T: 744 um/s, 9.11 Hz	2022-05-16 16:08:13 V: 1200 um/s, 6.81 Hz L: 549 um/s, 12.2 Hz T: 459 um/s, 6.38 Hz
2022-05-16 15:51:32	2022-05-16 15:51:32 V: 1710 um/s, 8.15 Hz L: 1340 um/s, 8.23 Hz T: 779 um/s, 9.08 Hz	2022-05-16 15:51:32 V: 1860 um/s, 5.42 Hz L: 1530 um/s, 11.5 Hz T: 1390 um/s, 11.4 Hz	2022-05-16 15:51:32 V: 1260 um/s, 9.83 Hz L: 927 um/s, 10.3 Hz T: 626 um/s, 11.0 Hz
2022-05-16 15:50:00	2022-05-16 15:50:00 V: 1010 um/s, 12.6 Hz L: 611 um/s, 13.7 Hz T: 375 um/s, 9.61 Hz	2022-05-16 15:50:00 V: 767 um/s, 8.09 Hz L: 708 um/s, 13.5 Hz T: 895 um/s, 11.7 Hz	2022-05-16 15:50:00 V: 585 um/s, 8.41 Hz L: 378 um/s, 12.8 Hz T: 410 um/s, 7.19 Hz
2022-05-16 15:37:55	2022-05-16 15:37:55 V: 313 um/s, 10.6 Hz L: 143 um/s, 6.33 Hz T: 139 um/s, 17.4 Hz	2022-05-16 15:37:55 V: 310 um/s, 7.21 Hz L: 185 um/s, 8.83 Hz T: 185 um/s, 7.23 Hz	2022-05-16 15:37:55 V: 183 um/s, 7.14 Hz L: 96 um/s, 8.45 Hz T: 97 um/s, 7.45 Hz

Transientrapport

Datum/Tid	MP_1 - V12	MP_2 - V12	MP_3 - V12
2022-05-16 15:21:41	2022-05-16 15:21:41 V: 236 um/s, 7.78 Hz L: 122 um/s, 29.7 Hz T: 151 um/s, 7.93 Hz	2022-05-16 15:21:41 V: 291 um/s, 7.35 Hz L: 192 um/s, 7.66 Hz T: 200 um/s, 7.52 Hz	2022-05-16 15:21:41 V: 91 um/s, 6.63 Hz L: 81 um/s, 7.62 Hz T: 77 um/s, 6.26 Hz
2022-05-16 15:10:11	2022-05-16 15:10:11 V: 895 um/s, 10.6 Hz L: 615 um/s, 7.32 Hz T: 261 um/s, 8.88 Hz	2022-05-16 15:10:11 V: 712 um/s, 8.42 Hz L: 563 um/s, 10.6 Hz T: 418 um/s, 13.3 Hz	2022-05-16 15:10:11 V: 406 um/s, 9.88 Hz L: 332 um/s, 10.2 Hz T: 232 um/s, 10.4 Hz
2022-05-16 15:07:50	2022-05-16 15:07:50 V: 998 um/s, 14.7 Hz L: 624 um/s, 13.8 Hz T: 384 um/s, 5.28 Hz	2022-05-16 15:07:50 V: 755 um/s, 8.34 Hz L: 661 um/s, 13.7 Hz T: 894 um/s, 11.3 Hz	2022-05-16 15:07:50 V: 566 um/s, 8.38 Hz L: 337 um/s, 14.4 Hz T: 478 um/s, 7.26 Hz
2022-05-16 14:39:01	2022-05-16 14:39:01 V: 232 um/s, 9.42 Hz L: 106 um/s, 5.89 Hz T: 97 um/s, 6.27 Hz	2022-05-16 14:39:01 V: 252 um/s, 6.54 Hz L: 134 um/s, 9.25 Hz T: 176 um/s, 9.90 Hz	2022-05-16 14:39:01 V: 158 um/s, 5.88 Hz L: 75 um/s, 6.42 Hz T: 71 um/s, 9.22 Hz
2022-05-16 14:26:55	2022-05-16 14:26:55 V: 878 um/s, 12.8 Hz L: 490 um/s, 11.1 Hz T: 457 um/s, 10.7 Hz	2022-05-16 14:26:55 V: 691 um/s, 7.76 Hz L: 578 um/s, 13.1 Hz T: 941 um/s, 12.8 Hz	2022-05-16 14:26:55 V: 577 um/s, 9.11 Hz L: 245 um/s, 13.9 Hz T: 405 um/s, 7.06 Hz
2022-05-16 14:15:02	2022-05-16 14:15:02 V: 1290 um/s, 10.8 Hz L: 657 um/s, 10.0 Hz T: 540 um/s, 10.9 Hz	2022-05-16 14:15:02 V: 1140 um/s, 8.75 Hz L: 824 um/s, 12.9 Hz T: 1140 um/s, 11.7 Hz	2022-05-16 14:15:02 V: 788 um/s, 11.0 Hz L: 529 um/s, 11.1 Hz T: 779 um/s, 8.71 Hz
2022-05-16 14:07:27	2022-05-16 14:07:27 V: 1200 um/s, 9.77 Hz L: 841 um/s, 6.33 Hz T: 674 um/s, 12.3 Hz	2022-05-16 14:07:27 V: 978 um/s, 6.63 Hz L: 769 um/s, 10.9 Hz T: 1080 um/s, 10.9 Hz	2022-05-16 14:07:27 V: 939 um/s, 7.23 Hz L: 544 um/s, 12.3 Hz T: 357 um/s, 10.7 Hz
2022-05-16 13:52:14	2022-05-16 13:52:14 V: 1920 um/s, 7.86 Hz L: 1390 um/s, 8.48 Hz T: 817 um/s, 9.33 Hz	2022-05-16 13:52:14 V: 1910 um/s, 9.54 Hz L: 1660 um/s, 9.60 Hz T: 1280 um/s, 10.8 Hz	2022-05-16 13:52:14 V: 1330 um/s, 7.44 Hz L: 919 um/s, 13.7 Hz T: 687 um/s, 11.0 Hz
2022-05-16 13:51:30	2022-05-16 13:51:30 V: 104 um/s, 21.2 Hz L: 21 um/s, 13.8 Hz T: 10 um/s, 9.50 Hz	2022-05-16 13:51:30 V: 53 um/s, 11.7 Hz L: 11 um/s, 6.58 Hz T: 29 um/s, 16.7 Hz	2022-05-16 13:51:30 V: 7 um/s, 12.5 Hz L: 4 um/s, 11.3 Hz T: 5 um/s, 311 Hz

Transientrapport

Projekt	Markvib tåg Jim exjobb Lindhov
Projektansvarig	Gustav Vågfelt
Tidsspann	2022-05-20 14:45 - 2022-05-20 17:45 (Europe/Stockholm)

Mätpunkt	MP_1	MP_2	MP_3
Plats	-	-	-
Sensortyp	V12	V12	V12
S/N	3510	2980	20810
Logger S/N	1746	1746	1746
Senaste kalibrering	2021-04-23	2021-04-23	2020-10-13
Standard	Geophone 5000µm/s 5-500Hz	Geophone 5000µm/s 5-500Hz	Geophone 5000µm/s 5-500Hz
Enhet	um/s	um/s	um/s
Storhet	Velocity	Velocity	Velocity
Intervalltid	1 min	1 min	1 min

Datum/Tid	MP_1 - V12	MP_2 - V12	MP_3 - V12
2022-05-20 17:35:03	2022-05-20 17:35:03 V: 394 um/s, 43.0 Hz L: 199 um/s, 13.0 Hz T: 156 um/s, 48.4 Hz	2022-05-20 17:35:03 V: 226 um/s, 20.2 Hz L: 212 um/s, 16.1 Hz T: 214 um/s, 43.5 Hz	2022-05-20 17:35:03 V: 106 um/s, 16.2 Hz L: 88 um/s, 16.4 Hz T: 69 um/s, 30.1 Hz
2022-05-20 17:17:33	2022-05-20 17:17:33 V: 744 um/s, 37.7 Hz L: 460 um/s, 38.1 Hz	2022-05-20 17:17:33 V: 470 um/s, 35.5 Hz T: 288 um/s, 43.6 Hz	2022-05-20 17:17:33 V: 136 um/s, 38.3 Hz T: 124 um/s, 7.70 Hz
2022-05-20 17:09:56	2022-05-20 17:09:56 V: 382 um/s, 30.4 Hz L: 376 um/s, 36.4 Hz T: 340 um/s, 37.5 Hz	2022-05-20 17:09:56 L: 382 um/s, 30.6 Hz	2022-05-20 17:09:56 L: 117 um/s, 9.39 Hz T: 111 um/s, 14.1 Hz
2022-05-20 17:05:01	2022-05-20 17:05:01 V: 368 um/s, 47.1 Hz L: 281 um/s, 31.8 Hz T: 250 um/s, 48.5 Hz	2022-05-20 17:05:01 V: 216 um/s, 38.9 Hz T: 154 um/s, 39.3 Hz	2022-05-20 17:05:01 V: 99 um/s, 44.3 Hz L: 71 um/s, 14.4 Hz
2022-05-20 16:54:19	2022-05-20 16:54:19 V: 1440 um/s, 38.2 Hz T: 966 um/s, 39.0 Hz	2022-05-20 16:54:19 T: 479 um/s, 41.9 Hz	2022-05-20 16:54:19 V: 170 um/s, 30.6 Hz L: 181 um/s, 25.4 Hz T: 150 um/s, 15.1 Hz
2022-05-20 16:49:22	2022-05-20 16:49:22 V: 328 um/s, 45.3 Hz L: 260 um/s, 11.0 Hz T: 311 um/s, 40.6 Hz	2022-05-20 16:49:22 V: 204 um/s, 41.9 Hz L: 251 um/s, 36.9 Hz	2022-05-20 16:49:22 V: 122 um/s, 44.2 Hz L: 75 um/s, 16.5 Hz
2022-05-20 16:33:59	2022-05-20 16:33:59 V: 1630 um/s, 39.0 Hz L: 1350 um/s, 30.9 Hz T: 954 um/s, 18.2 Hz		2022-05-20 16:33:59 V: 252 um/s, 14.7 Hz L: 302 um/s, 8.62 Hz
2022-05-20 16:33:28	2022-05-20 16:33:28 V: 106 um/s, 15.7 Hz L: 48 um/s, 76.8 Hz T: 83 um/s, 20.0 Hz	2022-05-20 16:33:28 V: 12 um/s, 19.6 Hz L: 4 um/s, 17.3 Hz T: 5 um/s, 11.4 Hz	2022-05-20 16:33:28 V: 4 um/s, 15.0 Hz L: 3 um/s, 367 Hz T: 6 um/s, 15.3 Hz
2022-05-20 16:26:54	2022-05-20 16:26:54 V: 672 um/s, 39.5 Hz L: 589 um/s, 42.0 Hz T: 569 um/s, 47.5 Hz	2022-05-20 16:26:54 V: 384 um/s, 38.0 Hz L: 318 um/s, 23.0 Hz T: 377 um/s, 31.1 Hz	2022-05-20 16:26:54 V: 169 um/s, 26.2 Hz L: 163 um/s, 10.7 Hz T: 145 um/s, 15.6 Hz
2022-05-20 16:22:32	2022-05-20 16:22:32 V: 1070 um/s, 41.7 Hz L: 465 um/s, 15.4 Hz T: 586 um/s, 44.7 Hz	2022-05-20 16:22:32 V: 499 um/s, 39.5 Hz L: 373 um/s, 37.3 Hz T: 373 um/s, 45.7 Hz	2022-05-20 16:22:32 V: 233 um/s, 18.1 Hz L: 155 um/s, 13.8 Hz T: 155 um/s, 13.6 Hz

Transientrapport

Datum/Tid	MP_1 - V12	MP_2 - V12	MP_3 - V12
2022-05-20 16:10:32	2022-05-20 16:10:32 V: 617 um/s, 45.4 Hz L: 651 um/s, 38.6 Hz T: 567 um/s, 44.3 Hz	2022-05-20 16:10:32 V: 306 um/s, 39.5 Hz L: 365 um/s, 25.9 Hz T: 310 um/s, 37.2 Hz	2022-05-20 16:10:32 V: 139 um/s, 16.4 Hz L: 168 um/s, 9.46 Hz T: 125 um/s, 14.5 Hz
2022-05-20 15:59:43	2022-05-20 15:59:43 V: 541 um/s, 24.1 Hz L: 341 um/s, 15.3 Hz T: 270 um/s, 34.8 Hz	2022-05-20 15:59:43 V: 294 um/s, 22.2 Hz L: 368 um/s, 12.4 Hz T: 261 um/s, 16.4 Hz	2022-05-20 15:59:43 V: 130 um/s, 14.3 Hz L: 114 um/s, 8.17 Hz T: 131 um/s, 8.89 Hz
2022-05-20 15:49:35	2022-05-20 15:49:35 V: 444 um/s, 44.6 Hz L: 276 um/s, 40.4 Hz T: 318 um/s, 43.0 Hz	2022-05-20 15:49:35 V: 255 um/s, 38.5 Hz L: 257 um/s, 35.9 Hz T: 225 um/s, 42.3 Hz	2022-05-20 15:49:35 V: 101 um/s, 37.2 Hz L: 90 um/s, 13.6 Hz T: 81 um/s, 6.45 Hz
2022-05-20 15:41:53	2022-05-20 15:41:53 V: 1070 um/s, 37.7 Hz L: 781 um/s, 43.8 Hz T: 721 um/s, 41.2 Hz	2022-05-20 15:41:53 V: 480 um/s, 32.9 Hz L: 469 um/s, 35.0 Hz T: 369 um/s, 29.5 Hz	2022-05-20 15:41:53 V: 162 um/s, 38.7 Hz L: 165 um/s, 24.8 Hz T: 134 um/s, 9.12 Hz
2022-05-20 15:22:07	2022-05-20 15:22:07 V: 593 um/s, 27.7 Hz L: 450 um/s, 37.7 Hz T: 309 um/s, 23.1 Hz	2022-05-20 15:22:07 V: 399 um/s, 27.0 Hz L: 227 um/s, 19.4 Hz T: 225 um/s, 25.4 Hz	2022-05-20 15:22:07 V: 97 um/s, 22.5 Hz L: 97 um/s, 21.5 Hz T: 135 um/s, 23.8 Hz
2022-05-20 15:15:40	2022-05-20 15:15:40 V: 485 um/s, 34.2 Hz L: 295 um/s, 51.2 Hz T: 301 um/s, 53.5 Hz		
2022-05-20 15:15:20	2022-05-20 15:15:20 V: 740 um/s, 29.5 Hz L: 645 um/s, 58.3 Hz T: 546 um/s, 25.7 Hz	2022-05-20 15:15:20 V: 384 um/s, 28.0 Hz L: 374 um/s, 26.6 Hz T: 360 um/s, 28.5 Hz	2022-05-20 15:15:20 V: 150 um/s, 26.3 Hz L: 172 um/s, 24.9 Hz T: 257 um/s, 7.58 Hz
2022-05-20 15:10:56	2022-05-20 15:10:56 V: 392 um/s, 36.1 Hz L: 273 um/s, 18.8 Hz T: 265 um/s, 44.0 Hz	2022-05-20 15:10:56 V: 162 um/s, 27.3 Hz L: 132 um/s, 24.8 Hz T: 143 um/s, 23.6 Hz	2022-05-20 15:10:56 V: 58 um/s, 28.6 Hz L: 67 um/s, 24.9 Hz T: 76 um/s, 9.93 Hz
2022-05-20 15:06:59	2022-05-20 15:06:59 V: 469 um/s, 42.1 Hz L: 239 um/s, 35.5 Hz T: 244 um/s, 37.2 Hz	2022-05-20 15:06:59 V: 520 um/s, 40.6 Hz L: 301 um/s, 39.7 Hz T: 297 um/s, 39.8 Hz	2022-05-20 15:06:59 V: 113 um/s, 27.8 Hz L: 86 um/s, 38.8 Hz T: 67 um/s, 23.8 Hz
2022-05-20 14:53:21	2022-05-20 14:53:21 V: 676 um/s, 31.7 Hz L: 567 um/s, 33.5 Hz T: 463 um/s, 35.1 Hz	2022-05-20 14:53:21 V: 323 um/s, 29.1 Hz L: 446 um/s, 34.1 Hz T: 284 um/s, 21.3 Hz	2022-05-20 14:53:21 V: 157 um/s, 24.9 Hz L: 222 um/s, 21.6 Hz T: 135 um/s, 29.7 Hz
2022-05-20 14:50:38	2022-05-20 14:50:38 V: 334 um/s, 32.9 Hz L: 120 um/s, 33.0 Hz T: 153 um/s, 35.9 Hz	2022-05-20 14:50:38 V: 119 um/s, 32.0 Hz L: 88 um/s, 30.5 Hz T: 102 um/s, 33.6 Hz	2022-05-20 14:50:38 V: 44 um/s, 25.3 Hz L: 55 um/s, 7.92 Hz T: 50 um/s, 26.2 Hz

DEPARTMENT OF SOME SUBJECT OR TECHNOLOGY
CHALMERS UNIVERSITY OF TECHNOLOGY
Gothenburg, Sweden
www.chalmers.se

CHALMERS
UNIVERSITY OF TECHNOLOGY